JEM Journal of Experimental Medicine

ARTICLE

Tcf1 and Lef1 are required for the immunosuppressive function of regulatory T cells

Shaojun Xing[1,2*], Kexin Gai[1*], Xiang Li[3], Peng Shao[1], Zhouhao Zeng[3], Xudong Zhao[4], Xin Zhao[1], Xia Chen[1], William J. Paradee[5], David K. Meyerholz[6], Weiqun Peng[3], and Hai-Hui Xue[1,7]

Tcf1 and Lef1 have versatile functions in regulating T cell development and differentiation, but intrinsic requirements for these factors in regulatory T (T reg) cells remain to be unequivocally defined. Specific ablation of Tcf1 and Lef1 in T reg cells resulted in spontaneous multi-organ autoimmunity that became more evident with age. Tcf1/Lef1-deficient T regs showed reduced protection against experimentally induced colitis, indicative of diminished immuno-suppressive capacity. Transcriptomic analysis revealed that Tcf1 and Lef1 were responsible for positive regulation of a subset of T reg–overrepresented signature genes such as *Ikzf4* and *Izumo1r*. Unexpectedly, Tcf1 and Lef1 were necessary for restraining expression of cytotoxic CD8⁺ effector T cell–associated genes in T reg cells, including *Prdm1* and *Ifng*. Tcf1 ChIP-seq revealed substantial overlap between Tcf1 and Foxp3 binding peaks in the T reg cell genome, with Tcf1-Foxp3 cooccupancy observed at key T reg signature and cytotoxic effector genes. Our data collectively indicate that Tcf1 and Lef1 are critical for sustaining T reg suppressive functions and preventing loss of self-tolerance.

Introduction

Regulatory T (T reg) cells are a subset of CD4⁺ T cells that are crucial for maintenance of immune tolerance and prevention of autoimmunity (Sakaguchi et al., 2013; Ramsdell and Ziegler, 2014). Compared with conventional CD4⁺ T (T conv) cells, T reg cells express the lineage-defining transcription factor Foxp3, and the expression of Foxp3 is subject to complex control by dozens of transcription factors and epigenetic regulators through at least four conserved noncoding sequences in or adjacent to the gene locus (Zheng et al., 2010; Lu et al., 2017; Zhao and Xue, 2017). It is also well established that Foxp3 does not act alone, and a myriad of cofactors engaging in transcriptional and epigenetic regulations have been identified to interact with Foxp3 through high-throughput screening or interaction mapping (Hori, 2012; Delacher et al., 2014). Foxp3, together with its interacting partners, forms large regulatory protein complexes to establish and maintain the T reg signature genes in a gene context–dependent manner. Given the complex protein–protein and protein–DNA interactions revolving around Foxp3, detailed dissection of such molecular interactions is necessary to advance our understanding of T reg cell biology and its contribution to pathophysiology in autoimmune disorders.

Tcf1 and Lef1 are transcription factors in the high-mobility group (HMG) family, and both have highly conserved HMG DNA binding domains (Staal and Sen, 2008; Xue and Zhao, 2012). Tcf1 and Lef1 are known for their regulatory roles in specifying thymic progenitors to the T cell lineage, instructing CD4⁺ T cell lineage choice, and establishing CD8⁺ T cell identity (Steinke and Xue, 2014; De Obaldia and Bhandoola, 2015). In many biological processes in which both factors are involved, Tcf1 and Lef1 frequently show functional redundancy, while Tcf1 exhibits a more predominant role (Steinke and Xue, 2014). In mature CD4⁺ T cells, Tcf1 is involved in multiple regulatory functions in differentiation of distinct helper lineages, promoting T helper 2 (Th2) and follicular helper T (Tfh) but repressing Th1 and Th17 formation (Yu et al., 2009; Choi et al., 2015; Wu et al., 2015; Xu et al., 2015; Zhang et al., 2018). However, a role of Tcf1 and Lef1 in T reg cells has not been definitively defined.

In systematic characterization of T reg signature genes, Tcf1 and Lef1 are found among genes that are underexpressed in T reg compared with T conv cells, considered to be among T reg–down signature genes (Hill et al., 2007; Fu et al., 2012). The lower expression of Tcf1 and Lef1 on protein levels was

[1]Departments of Microbiology and Immunology, Carver College of Medicine, University of Iowa, Iowa City, IA; [2]Guangdong Key Laboratory of Regional Immunity and Diseases, Department of Pathogen Biology, Shenzhen University School of Medicine, Shenzhen, Guangdong, China; [3]Department of Physics, The George Washington University, Washington DC; [4]Department of Otorhinolaryngology, Shengjing Hospital, China Medical University, Shenyang, China; [5]Genome Editing Core Facility, University of Iowa, Coralville, IA; [6]Department of Pathology, Carver College of Medicine, University of Iowa, Iowa City, IA; [7]Iowa City Veterans Affairs Health Care System, Iowa City, IA.

*S. Xing and K. Gai contributed equally to this work; Correspondence to Hai-Hui Xue: hai-hui-xue@uiowa.edu; Weiqun Peng: wpeng@gwu.edu.

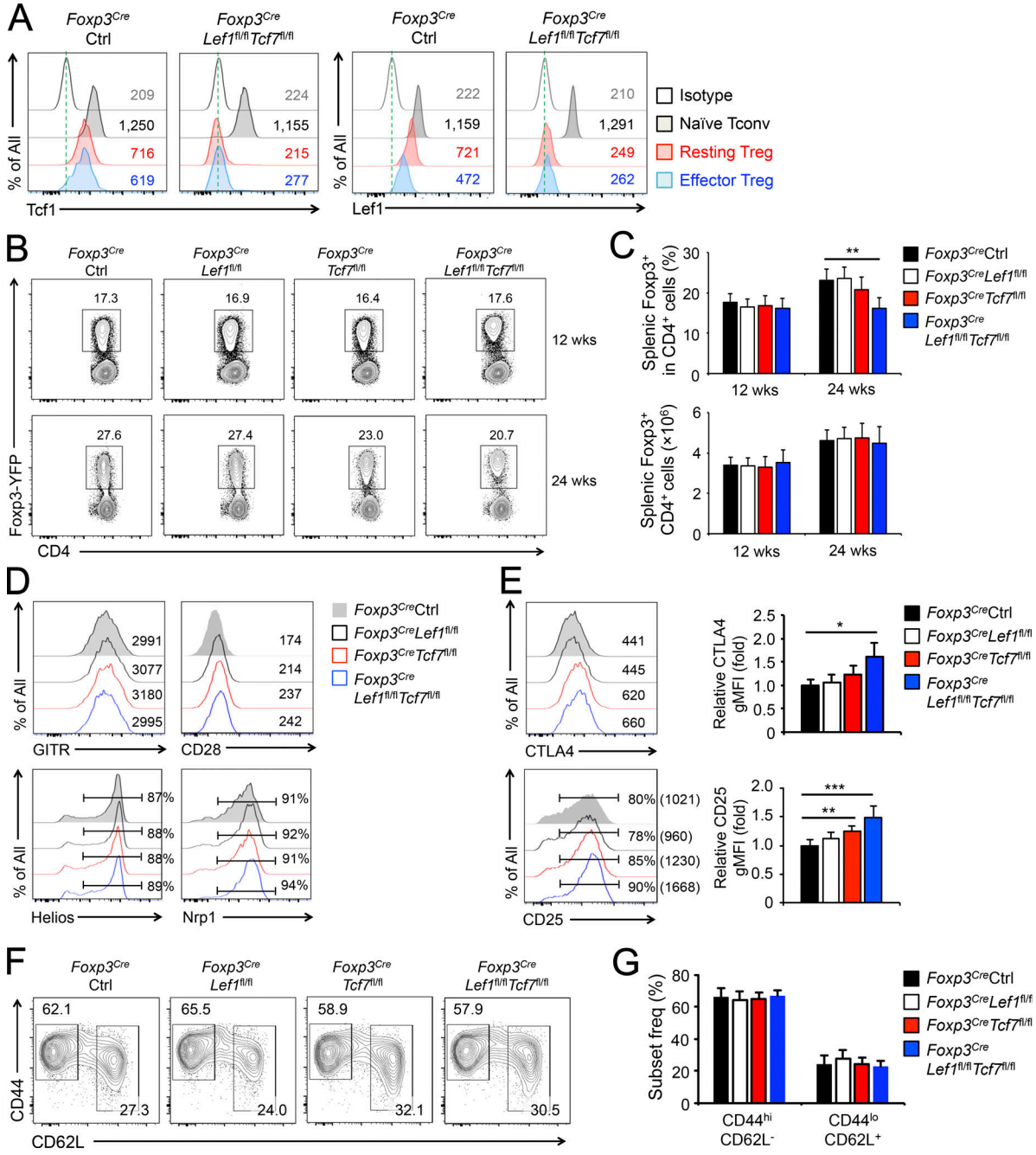

Figure 1. **Loss of Tcf1 and/or Lef1 does not detectably perturb T reg cell homeostasis. (A)** Detection of Tcf1 and Lef1 expression levels. Splenocytes from *Foxp3*^{Cre} control and *Foxp3*^{Cre}*Tcf7*$^{fl/fl}$*Lef1*$^{fl/fl}$ mice (5 wk old) were stained to identify TCRβ$^+$CD4$^+$CD25$^-$Foxp3$^-$ T conv and TCRβ$^+$CD4$^+$CD25$^+$Foxp3$^+$ T reg cells. Tcf1 and Lef1 were determined by intracellular staining in CD44^{lo}CD62L$^+$ naive T conv cells, CD44^{lo}CD62L$^+$ resting T reg, and CD44^{hi}CD62L$^-$ effector T reg cell subsets. Values denote geometric mean fluorescent intensity (gMFI), and dotted green lines mark gMFI of isotype control staining. Data are representative from two experiments with similar results. **(B and C)** Detection of T reg cells in the spleen. Spleens were harvested from mice of indicated genotypes at 12 or 24 wk of age, and Foxp3-YFP$^+$ cells were detected in TCRβ$^+$CD4$^+$ T cells, with representative data in B and cumulative data on the frequency (top) and numbers (bottom) of T reg cells in C. **(D and E)** Detection of key molecules on T reg cells. Splenic T reg cells from mice of indicated genotypes at ≥24 wk were analyzed for expression of GITR, CD28, and Nrp1 by cell surface staining and that of Helios and CTLA4 by intracellular staining. CD25 expression was detected on T reg cells from LNs. Values denote gMFI, and those in percentages denote the frequency of gated population. Cumulative data on gMFI of total CTLA and CD25 are in E. **(F and G)** Detection of effector and resting T reg cells. Splenic T reg cells were subfractionated to CD44^{hi}CD62L$^-$ effector T reg and CD44^{lo}CD62L$^+$ resting T reg subsets, with representative data in F and cumulative data on subset frequency in G. Data are means ± SD from more than four independent experiments (n ≥ 9 for each group). Statistical significance in C, E, and G was determined by one-way ANOVA, followed by Student's t test for indicated pairwise comparisons. *, P < 0.05; **, P < 0.01; ***, P < 0.001.

independently confirmed using mass spectrometry (Barra et al., 2015), and in line with these observations, the *TCF7* gene locus, which encodes Tcf1, is more heavily methylated in human T reg than T conv cells (Baron et al., 2007). It is also suggested that Tcf1 may physically interact with Foxp3, and this interaction was reportedly enriched at the *Il2* promoter for transcriptional repression using in vitro assays (van Loosdregt et al., 2013). Using computational network inference approach, Fu et al. (2012) predicted that Lef1 is one of transcription factors that cooperate with Foxp3 and is responsible for the expression of a portion of T reg signature genes. Functional analyses using the germline-targeted *Tcf7* mouse strain showed that loss of Tcf1 appeared to allow precursor T cells with lower TCR affinity to self-peptides to develop into T reg cells (Barra et al., 2015), and Tcf1-deficient T reg cells seemed to more effectively inhibit proliferation of activated T conv $CD4^+$ T cells as determined by an in vitro suppression assay (van Loosdregt et al., 2013). These reported results generate an overall impression that Tcf1 and Lef1 may function as negative regulators of T reg suppressive functions.

Tcf1 has developmental stage–specific effects during T cell development and lineage-specific effects in helper $CD4^+$ and cytotoxic $CD8^+$ T cells (Xue and Zhao, 2012; He et al., 2016; Shan et al., 2017). To specifically address the functional requirements for Tcf1 and Lef1, we ablated both genes using the *Foxp3* locus-driven Cre recombinase and found loss of self-tolerance in mice at advanced ages. Mechanistic analysis further revealed co-occupancy of Tcf1 and Foxp3 at a portion of T reg signature gene loci and an unexpected role of Tcf1 and Lef1 in restraining the expression of genes that are associated with cell cycle progression and $CD8^+$ effectors in T reg cells. Our data indicate that Tcf1 and Lef1 are important contributors to maintaining the immunosuppressive functions in T reg cells, despite that their expression in T reg cells is not as high as that in T conv $CD4^+$ and $CD8^+$ T cells.

Results

Deficiency in Tcf1 and/or Lef1 does not perturb T reg cell homeostasis

Tcf1 and Lef1 are expressed at lower levels in T reg cells than T conv cells (Hill et al., 2007; Fu et al., 2012). By intracellular staining, Tcf1 and Lef1 expression were indeed detected at lower levels in T reg cells, and interestingly, their expression was further reduced in $CD44^{hi}CD62L^-$ effector T reg cells compared with $CD44^{lo}CD62L^+$ resting T reg cells (Fig. 1 A). To define the precise role of Tcf1 and Lef1 in T reg cells in vivo, we generated mice with T reg cell–specific deletion of *Tcf7* and/or *Lef1* by crossing $Tcf7^{fl/fl}$ or $Lef1^{fl/fl}$ strains established in our laboratory (Yu et al., 2012; Steinke et al., 2014) to $Foxp3^{Cre}$ mice, which express a fusion of YFP and Cre recombinase under the control of *Foxp3* locus (Rubtsov et al., 2008). We confirmed specific deletion of Tcf1 and Lef1 proteins in all T reg subsets but not T conv $CD4^+$ cells in $Foxp3^{Cre}Tcf7^{fl/fl}Lef1^{fl/fl}$ mice (Fig. 1 A). Deletion of either Tcf1 and/or Lef1 did not detectably affect the numbers of $Foxp3^+$ T reg cells in the thymus or spleen at 12 or 24 wk of age, whereas deletion of both factors modestly affected the frequency of T reg cells (Fig. 1, B and C; and Fig. S1). Phenotypic analysis of mice at ≥24 wk showed that T reg cells expressed similar levels of T reg–associated proteins such as CD28 and GITR, and similar portions of T reg cells expressed Helios and neuropilin-1 (Nrp1) among mice of all four genotypes (Fig. 1 D). On the other hand, CTLA4 and CD25 were detected at modestly increased levels on T reg cells from $Foxp3^{Cre}Tcf7^{fl/fl}Lef1^{fl/fl}$ mice than those from $Foxp3^{Cre}$ control mice (Fig. 1 E). In addition, the resting and effector T reg cells were detected at similar frequency among all four genotypes (Fig. 1, F and G). Although Tcf1 and Lef1 expression was higher in the resting T reg cells, ablation of Tcf1 and/or Lef1 did not detectably alter the distribution of T reg cells in resting and effector subsets. These data demonstrate that deficiency in Tcf1 and/or Lef1 did not perturb T reg pool size or phenotypes under homeostatic conditions.

Loss of Tcf1 and Lef1 leads to aberrant T cell activation and autoimmunity

To investigate if ablating Tcf1 and/or Lef1 in T reg cells disrupts T reg cell function in vivo, we tracked mice over time. Both female and male $Foxp3^{Cre}Tcf7^{fl/fl}Lef1^{fl/fl}$ mice showed progressive weight loss after 12 wk of age (Fig. 2 A). The weight loss was less pronounced in $Foxp3^{Cre}Tcf7^{fl/fl}$ mice, reaching statistical significance only at 24 wk of age, whereas $Foxp3^{Cre}Lef1^{fl/fl}$ mice showed similar growth rate with $Foxp3^{Cre}$ control mice (Fig. 2 A). The aged $Foxp3^{Cre}Tcf7^{fl/fl}Lef1^{fl/fl}$ mice also manifested autoimmune symptoms such as hair loss and scaly tails. In the peripheral lymphoid organs, both T conv Foxp3-YFP^-CD4^+ and $CD8^+$ T cells showed increased frequency and numbers in $CD44^{hi}CD62L^-$ activated phenotype, with concordant reduction in $CD44^{lo}CD62L^+$ naive phenotype, in $Foxp3^{Cre}Tcf7^{fl/fl}Lef1^{fl/fl}$ mice at 24 wk of age (Fig. 2, B and C). In addition, both T conv YFP^-CD4^+ and $CD8^+$ T cells in aged $Foxp3^{Cre}Tcf7^{fl/fl}Lef1^{fl/fl}$ mice showed increased proliferation (Fig. S2, A and B) and enhanced IFN-γ production (Fig. 2, D and E). In contrast, the aberrant T cell activation and excessive IFN-γ production were not observed in $Foxp3^{Cre}Tcf7^{fl/fl}Lef1^{fl/fl}$ mice at 8–12 wk of age (Fig. S2, C and D). These data suggest deteriorating suppressive functions in T reg cells lacking Tcf1 and Lef1 in vivo with aging. It is also of note that $Foxp3^{Cre}Lef1^{fl/fl}$ and control mice were phenotypically similar, and T cell activation phenotypes in $Foxp3^{Cre}Tcf7^{fl/fl}$ mice were observed but not as pronounced as those in $Foxp3^{Cre}Tcf7^{fl/fl}Lef1^{fl/fl}$ mice (Fig. 2, B–E), indicating functional redundancy between Tcf1 and Lef1 in T reg cells. We also examined nonlymphoid organs and found increased infiltrates of mononuclear immune cells, especially in the lung and small intestines in aged $Foxp3^{Cre}Tcf7^{fl/fl}$ and $Foxp3^{Cre}$ $Tcf7^{fl/fl}Lef1^{fl/fl}$ mice (Fig. 2, F and G). These findings indicate that Tcf1/Lef1-deficient T reg cells failed to maintain immune homeostasis, albeit they were present in expected frequency and appeared to express normal levels of a few known T reg proteins.

Tcf1/Lef1-deficient T reg cells are functionally impaired

We next directly investigated if Tcf1 and Lef1 are required for the immunosuppressive function of T reg cells. Because aberrant T cell activation and multitissue inflammation were most pronounced in the absence of both factors, most of our analyses

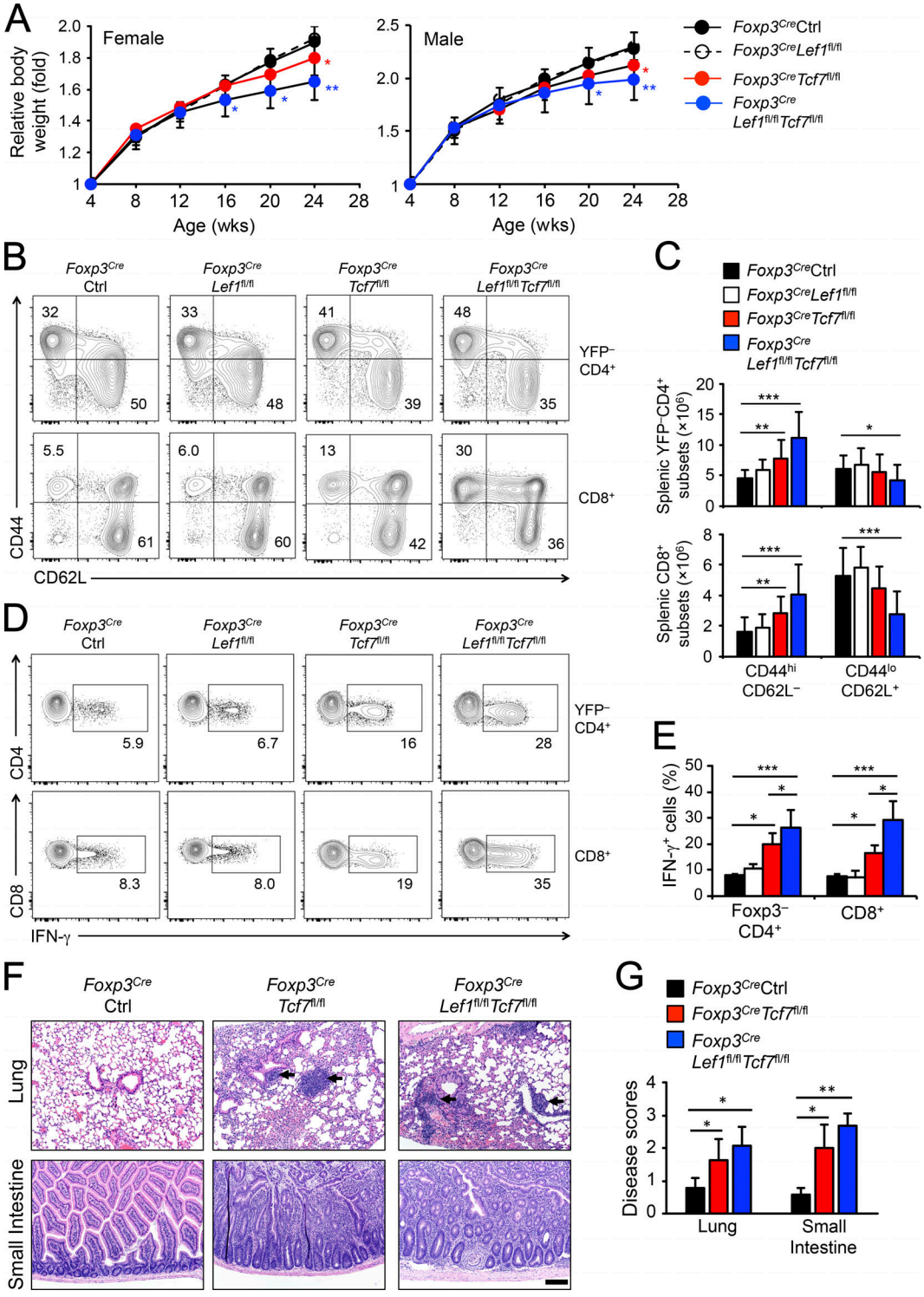

Figure 2. **Ablating Tcf1 and Lef1 in T reg cells results in loss of self-tolerance. (A)** Tracking body weight of female and male mice of indicated genotypes at 4-wk intervals. Data are means ± SD ($n \geq 9$ for each group). *, $P < 0.05$; **, $P < 0.01$ by Student's *t* test compared with *Foxp3*^{Cre} control mice. **(B and C)** Detection of activation status of T cells. Spleens were harvested from mice of indicated genotypes at ≥24 wk, and T conv YFP$^-$CD4$^+$ and CD8$^+$ T cells were analyzed for CD44^{hi}CD62L$^-$ effector and CD44^{lo}CD62L$^+$ naive subsets, with representative data in B and cumulative data on the frequency (top) and numbers (bottom) of each subset of cells in C. **(D and E)** IFN-γ production by splenic YFP$^-$CD4$^+$ and CD8$^+$ T cells from mice of indicated genotypes at ≥24 wk, with representative data in D and cumulative data in E. Data in C and E are means ± SD from more than four independent experiments ($n \geq 9$ for each group). **(F and G)** Histology of lung and small intestine from mice of indicated genotypes at ≥24 wk of age. Tissue sections were stained with hematoxylin and eosin. **(F)** Representative images ($n \geq 6$ for each genotype). Arrows mark perivascular and interstitial leukocyte aggregates in lung. Inflammatory infiltrates expanded the lamina propria of the small intestine in the right two panels. Bar, 140 µm. **(G)** Cumulative disease scores are means ± SD. Statistical significance in C, E, and G was determined by one way ANOVA, followed by Student's *t* test for indicated pairwise comparisons. *, $P < 0.05$; **, $P < 0.01$; ***, $P < 0.001$.

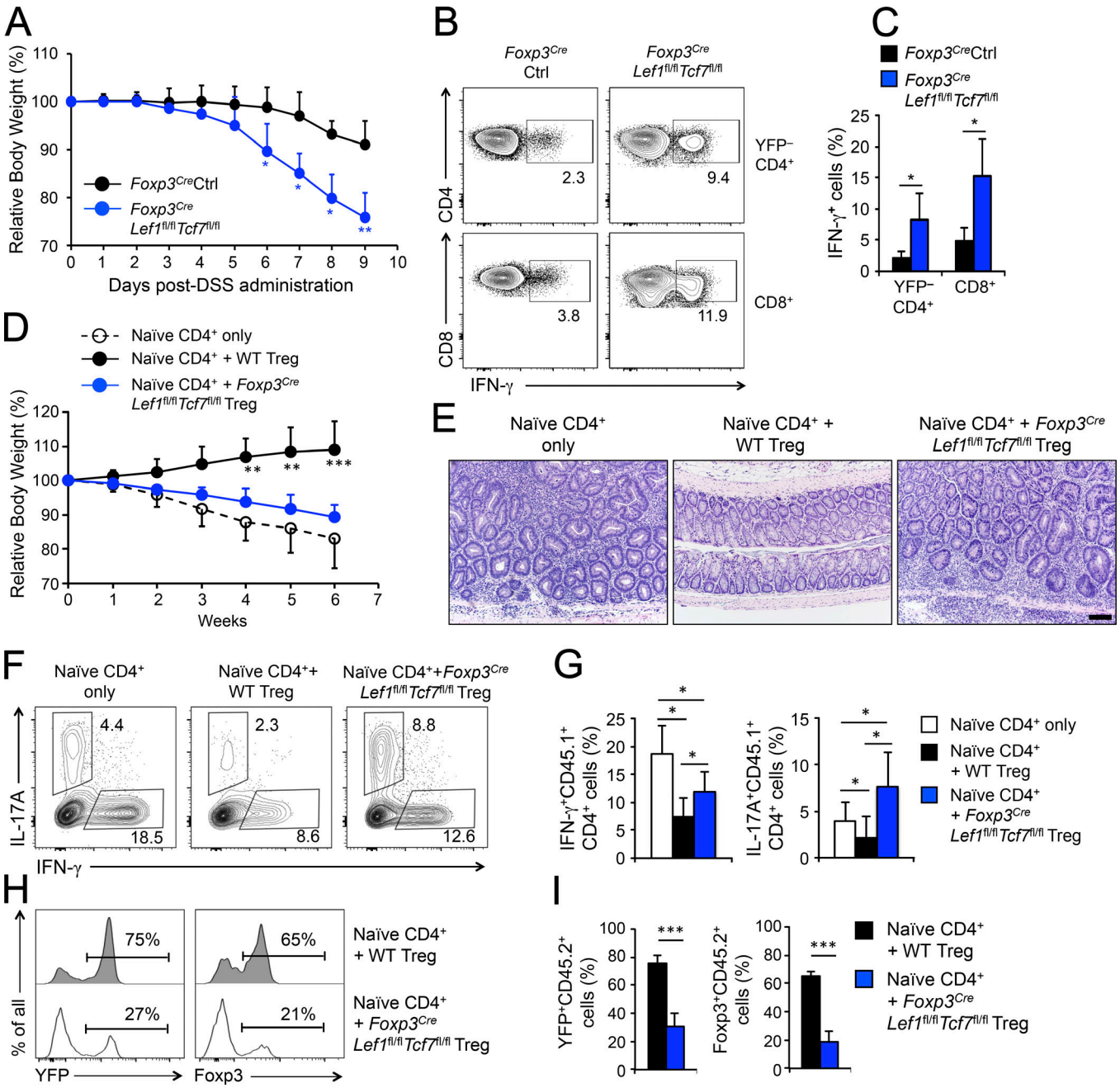

Figure 3. **Tcf1/Lef1-deficient T reg cells are functionally impaired. (A–C)** DSS-induced acute colitis model. *Foxp3*^{Cre}*Tcf7*$^{fl/fl}$*Lef1*$^{fl/fl}$ and *Foxp3*^{Cre} control mice at 6–12 wk were given DSS at 1.75 g/100 ml (1.75% wt/vol) in drinking water for 8 d and the body weight was tracked daily (A). On day 9, the mesenteric LNs were harvested, and T conv YFP$^-$CD4$^+$ and CD8$^+$ T cells were stimulated with anti-CD3 and anti-CD28 and measured for IFN-γ production. Representative data are in B, and cumulative data are in C. Data in A and C are means ± SD from two independent experiments (n = 8 for control, and 5 for *Foxp3*^{Cre}*Tcf7*$^{fl/fl}$*Lef1*$^{fl/fl}$ mice). *, P < 0.05; **, P < 0.01 by Student's t test at indicated time points. **(D–I)** Chronic colitis model. CD25$^-$CD45RA$^+$ naive CD4$^+$ T cells were sorted from CD45.1$^+$ B6.SJL mice and adoptively transferred into *Rag1*$^{-/-}$ mice alone or together with CD25$^+$YFP$^+$ T reg cells sorted from *Foxp3*^{Cre} control or *Foxp3*^{Cre}*Tcf7*$^{fl/fl}$*Lef1*$^{fl/fl}$ mice at 6–12 wk old. The body weight of recipients was tracked weekly (D). Data are means ± SD from three independent experiments (n = 9–11 for each group). **, P < 0.01; ***, P < 0.001 compared with the naive CD4$^+$-only group by Student's t test. **(E)** Histology of colon. Colon sections from *Rag1*$^{-/-}$ recipients in each group were stained with hematoxylin and eosin. Inflammatory infiltrates expanded the lamina propria in right and left panels, but were lacking in the middle panel. Bar, 105 µm. **(F and G)** Cytokine production by CD45.1$^+$CD4$^+$ T cells from mesenteric LNs, with representative data in F and cumulative data in G. **(H and I)** Foxp3 expression in T reg cells in mesenteric LNs, as measured by YFP expression or intracellular staining for Foxp3, with representative data in H and cumulative data in I. Data in G and I are means ± SD from two independent experiments (n = 6 for each group). Statistical significance in G was determined by one way ANOVA, followed by Student's t test for indicated pairwise comparisons. *, P < 0.05; ***, P < 0.001.

focused on T reg cells from *Foxp3*^{Cre}*Tcf7*$^{fl/fl}$*Lef1*$^{fl/fl}$ mice. The inflammatory manifestation in *Foxp3*^{Cre}*Tcf7*$^{fl/fl}$*Lef1*$^{fl/fl}$ mice was more evident in aged mice, and thus suggested progressive functional impairment in T reg cells. Based on this reasoning, we specifically analyzed T reg cells in mice 6–12 wk old to avoid potential secondary effects. In vitro suppression assay showed that splenic T regs cells from WT and *Foxp3*^{Cre}*Tcf7*$^{fl/fl}$*Lef1*$^{fl/fl}$ mice had similar capacity in suppressing proliferation of T conv CD4$^+$ effector T cells (Fig. S2 E). We then tested an acute colitis model induced by dextran sodium sulfate (DSS), which causes intestinal mucus to become permeable to luminal bacterial antigens and evokes T cell responses (Morgan et al., 2013). We titrated the DSS dosage to allow colitis to develop but at a slower rate in *Foxp3*^{Cre} control mice, and under this condition, *Foxp3*^{Cre}*Tcf7*$^{fl/fl}$*Lef1*$^{fl/fl}$ mice exhibited exacerbated weight loss than *Foxp3*^{Cre} control littermates (Fig. 3 A). In addition, both T conv CD4$^+$ and CD8$^+$ T cells from the draining mesenteric LNs of DSS-treated *Foxp3*^{Cre}*Tcf7*$^{fl/fl}$*Lef1*$^{fl/fl}$ mice showed increased portion in activated, effector phenotypes (Fig. S2, F and G) and elevated IFN-γ production (Fig. 3, B and C), suggesting diminished T reg function in the absence of Tcf1 and Lef1.

To further substantiate the requirement for Tcf1 and Lef1 in T reg cell function, we next used a chronic colitis model. We adoptively transferred CD45.1$^+$ congenic naive T conv CD4$^+$ T cells into *Rag1*$^{-/-}$ mice alone or together with T reg cells from *Foxp3*^{Cre}*Tcf7*$^{fl/fl}$*Lef1*$^{fl/fl}$ or *Foxp3*^{Cre} control mice. As expected, the transfer of naive T cells alone caused progressive weight loss and massive infiltration of inflammatory cells, and cotransfer with T reg cells from *Foxp3*^{Cre} control mice prevented weight loss and colon pathology (Fig. 3, D and E). In contrast, T reg cells from *Foxp3*^{Cre}*Tcf7*$^{fl/fl}$*Lef1*$^{fl/fl}$ mice failed to suppress the disease (Fig. 3, D and E). In the draining mesenteric LNs, a substantial portion of the CD45.1$^+$CD4$^+$ T cells produced IL-17A or IFN-γ when the naive CD4$^+$ T cells were transferred alone, and these cytokine-producing cells were substantially reduced when control T reg cells were transferred together (Fig. 3, F and G). However, cotransfer of T reg cells from *Foxp3*^{Cre}*Tcf7*$^{fl/fl}$*Lef1*$^{fl/fl}$ mice only modestly reduced the frequency of IFN-γ–producing but somehow increased that of IL-17A–producing CD4$^+$ T cells (Fig. 3, F and G). On the other hand, the control T reg cells in the mesenteric LNs were mostly maintained for active transcription of the *Foxp3* gene (as measured by the YFP reporter) and Foxp3 protein expression; in contrast, a much smaller portion of Tcf1/Lef1-deficient T reg cells maintained active Foxp3 transcription and protein expression (Fig. 3, H and I). These in vivo data collectively indicate that Tcf1 and Lef1 are critical for the suppressive function of T reg cells.

Tcf1 and Lef1 synergize with T-bet in regulating T reg suppressive function

While performing phenotypic analysis of T reg cells from *Foxp3*^{Cre}*Tcf7*$^{fl/fl}$*Lef1*$^{fl/fl}$ or *Foxp3*^{Cre} control mice, we noticed that Tcf1/Lef1-deficent T reg cells exhibited increased CXCR3 expression (Fig. 4 A). T-bet is known to induce CXCR3 expression (Koch et al., 2009), and the T-bet$^+$ subset of T reg cells confers unique protection against excessive Th1 and CD8$^+$ T cell responses to intracellular pathogens (Koch et al., 2012; Levine et al., 2017). Indeed, T-bet expression, as detected by intracellular staining, was elevated in *Foxp3*^{Cre}*Tcf7*$^{fl/fl}$*Lef1*$^{fl/fl}$ but was not evidently increased in *Foxp3*^{Cre}*Tcf7*$^{fl/fl}$ or *Foxp3*^{Cre}*Lef1*$^{fl/fl}$ T reg cells (Fig. 4 A). This observation suggests that T-bet might be upregulated as a compensatory mechanism to sustain T reg functions in the absence of Tcf1 and Lef1. It has been consistently observed that ablating T-bet in T reg cells caused only modest autoimmune phenotypes (Levine et al., 2017); however, combined deficiency in T-bet and Gata3 diminishes the suppressive capacity of T reg cells (Yu et al., 2015). We therefore hypothesized that T-bet might also synergize with Tcf1 and Lef1 in sustaining T reg functions.

To test this, we generated *Foxp3*^{Cre}*Tcf7*$^{fl/fl}$*Lef1*$^{fl/fl}$*Tbx21*$^{fl/fl}$ mice. At ≥24 wk, the triple-deficient mice had similar numbers of splenic T reg cells as *Foxp3*^{Cre}*Tcf7*$^{fl/fl}$*Lef1*$^{fl/fl}$ and *Foxp3*^{Cre} control mice (Fig. 4 B), and the distribution among resting (CD44^{lo}CD62L$^+$) and effector (CD44^{hi}CD62L$^-$) T reg compartments was also similar (Fig. 4 C). Upon stimulation ex vivo, increased portion of Tcf1/Lef1-deficient T reg cells produced IFN-γ compared with control cells, and this increase was abolished upon additional ablation of T-bet (Fig. 4 D). In spite of the apparently normal T reg cell numbers and the correction of IFN-γ production by T reg cells from the *Foxp3*^{Cre} *Tcf7*$^{fl/fl}$*Lef1*$^{fl/fl}$*Tbx21*$^{fl/fl}$ mice, Foxp3-YFP$^-$ T conv CD4$^+$ and CD8$^+$ T cells in these mice showed higher frequency and numbers in CD44^{hi}CD62L$^-$ activated phenotype and higher frequency in producing IFN-γ than those in *Foxp3*^{Cre}*Tcf7*$^{fl/fl}$*Lef1*$^{fl/fl}$ mice (Fig. 4, E and F). Collectively, these data indicate that abrogating the T-bet pathway exacerbated T reg cell defects caused by Tcf1/Lef1 deficiency and further substantiate the notion that Tcf1 and Lef1 function as positive regulators of T reg cell functions, in part through concerted action with T-bet.

Molecular targets of Tcf1 in T reg cells

To investigate the molecular mechanisms by which Tcf1 and Lef1 regulated T reg cells, we sort-purified T reg cells from *Foxp3*^{Cre}*Tcf7*$^{fl/fl}$*Lef1*$^{fl/fl}$ or *Foxp3*^{Cre} control mice for RNA sequencing (RNA-seq) analysis, in which male mice were used at 16 wk of age when autoimmune phenotypes were not evident (Fig. 2). We then analyzed the T reg cell transcriptomes with gene set enrichment analysis (GSEA), which assesses the behavior of the whole gene set rather than a preset fold change threshold. Using C2-curated gene sets in public domain, 133 gene sets were enriched in Tcf1/Lef1-deficient T reg cells with a nominal false discovery rate (FDR) at 0, and among these, 31 gene sets were associated with cell cycle regulation. For example, in the "REACTOME_CELL_CYCLE" gene set that contains 377 genes, 185 genes exhibited increased expression in Tcf1/Lef1-deficient T reg cells (Fig. 5 A). The "GOLDRATH_ANTIGEN_RESPONSE" gene set, defined as genes up-regulated in peak immune response by CD8$^+$ T cells (Goldrath et al., 2004), was unexpectedly enriched in Tcf1/Lef1-deficient T reg cells, showing increased expression of 203 genes of a total of 315 in the gene set (Fig. 5 B). These genes included *Gzmb* and *Prf1*, which encode cytotoxic molecules granzyme B and perforin, respectively, and *Prdm1*, encoding Blimp1 transcription factor that is critical for effector CD8$^+$ T cell function. Although up-regulated

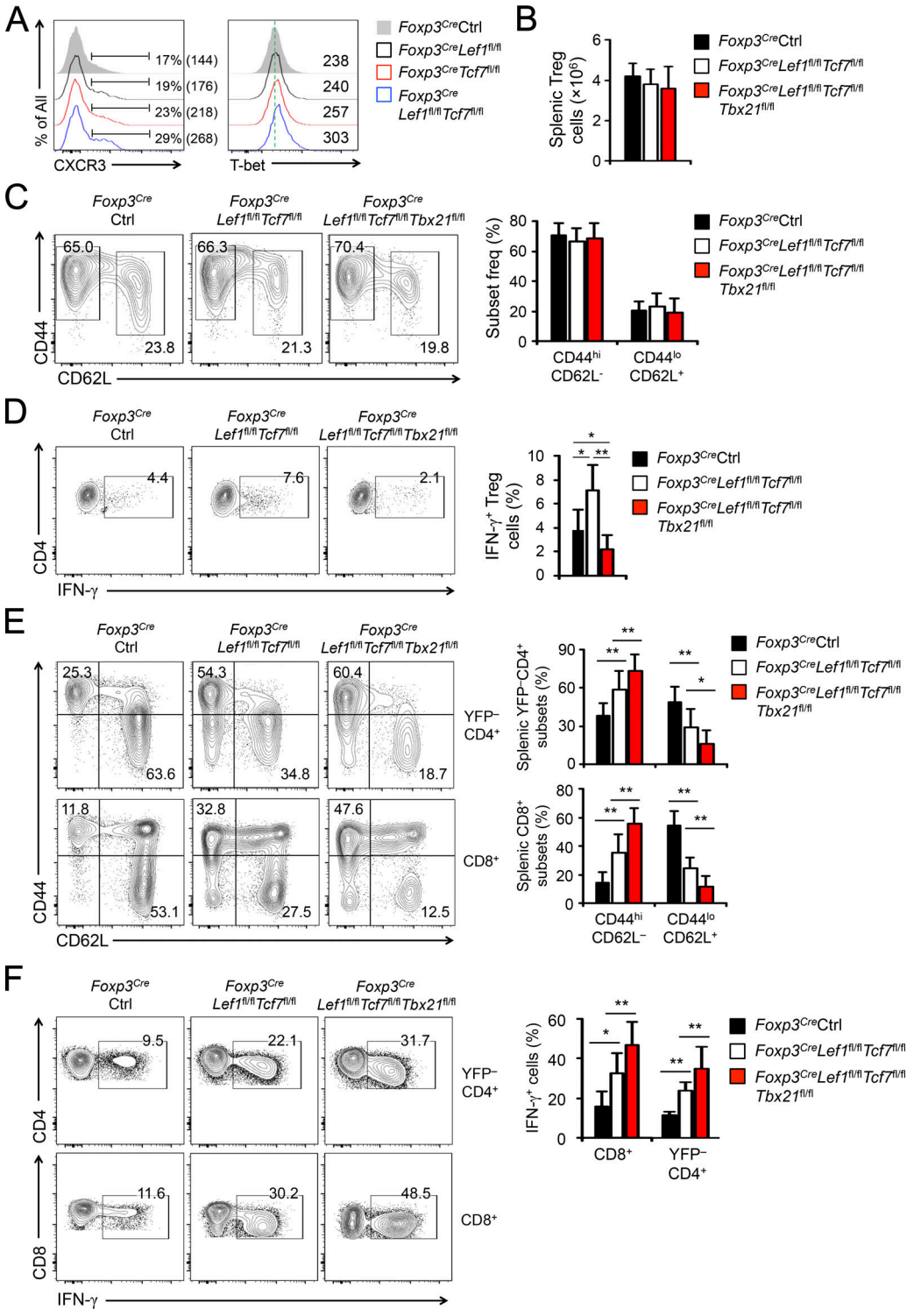

Figure 4. **Ablating T-bet in T reg cells exacerbates inflammatory responses in the absence of Tcf1 and Lef1. (A)** Detection of CXCR3 (surface) and T-bet (intracellular) expression in splenic T reg cells from mice of indicated genotypes at ≥24 wk. Values denote gMFI and those in percentages denote the frequency of gated population. Data are representative from three experiments with similar results. **(B)** Detection of Foxp3-YFP$^+$ T reg cells in the spleens from mice of indicated genotypes at ≥24 wk of age. Data are means ± SD ($n \geq 8$ for each group). **(C)** Detection of CD44^{hi}CD62L$^-$ effector and CD44^{lo}CD62L$^+$ resting T reg cells in spleens from mice of indicated genotypes at ≥24 wk of age. Representative data from three experiments are on the left, and cumulative data on subset frequency on the right are means ± SD from three experiments ($n \geq 8$ for each group). **(D)** IFN-γ production by splenic T reg cells, with representative data on the left and cumulative data on the right, showing means ± SD from three independent experiments ($n \geq 6$ for each group). **(E and F)** Detection of activation status and IFN-γ production by splenic YFP$^-$CD4$^+$ and CD8$^+$ T cells. Representative data are shown in left panels, and cumulative data are in right panels, showing the frequency of CD44^{hi}CD62L$^-$ effector and CD44^{lo}CD62L$^+$ naive subsets in YFP$^-$CD4$^+$ and CD8$^+$ T cells (top and bottom panels in E, respectively). The cumulative data are means ± SD from three independent experiments ($n \geq 8$ for each group). Statistical significance in B–F was determined by one way ANOVA, followed by Student's *t* test for indicated pairwise comparisons. *, $P < 0.05$; **, $P < 0.01$.

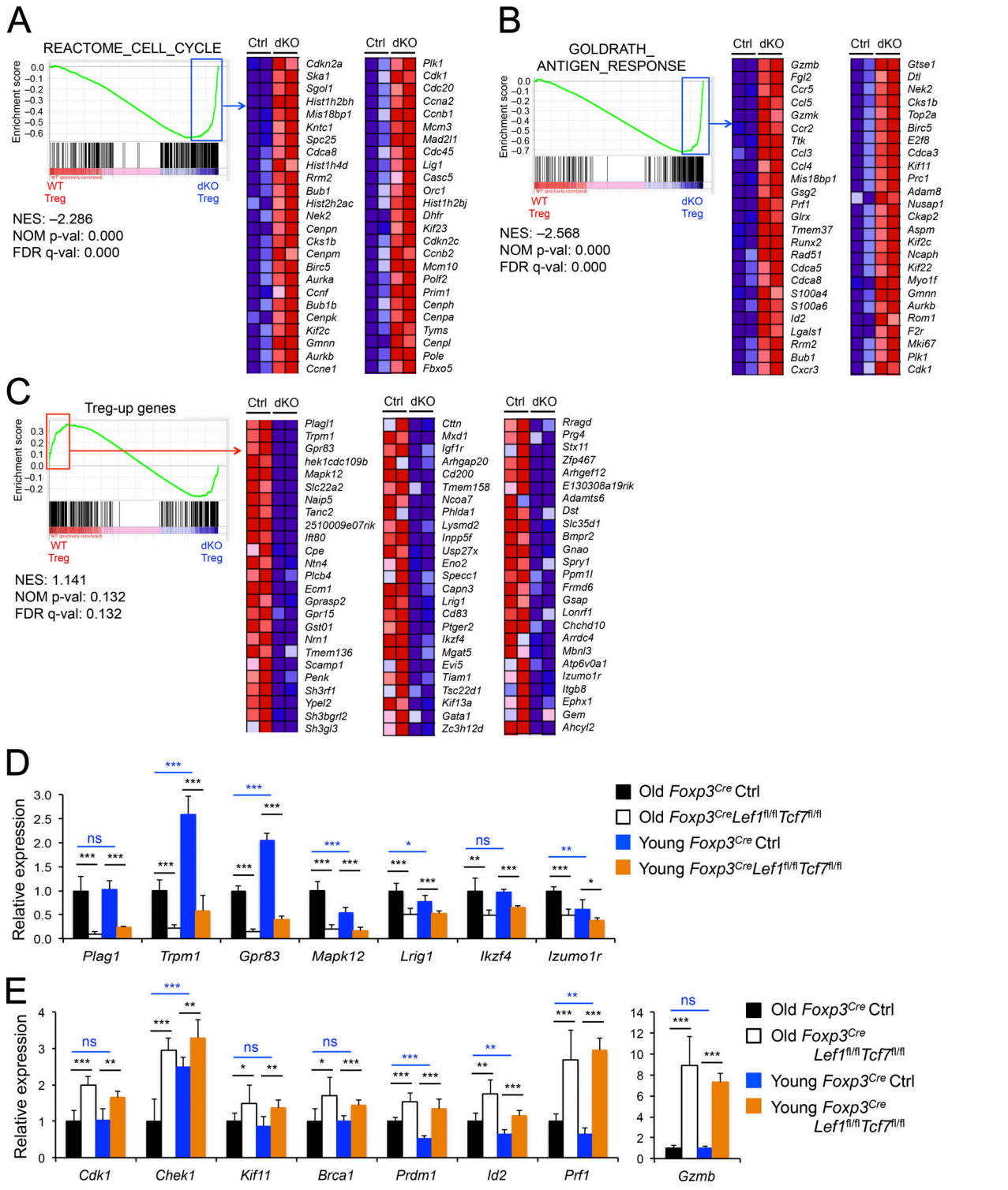

Figure 5. **Impact of Tcf1/Lef1 deficiency on T reg cell transcriptome. (A–C)** GSEA of transcriptomic changes of Tcf1/Lef1-deficient T reg cells. CD25^{+}YFP^{+} T reg cells were sorted from the spleens of male *Foxp3*^{Cre} control or *Foxp3*^{Cre}*Tcf7*$^{fl/fl}$*Lef1*$^{fl/fl}$ (dKO) mice at 16 wk of age and analyzed by RNA-seq, and the data were analyzed by GSEA C2-curated gene sets including "REACTOME_CELL_CYCLE" (A) and "GOLDRATH_ANTIGEN_RESPONSE" (B), and custom T reg–up signature gene set (C). Blue and red rectangles denote the leading edges of enrichment plots showing negative and positive enrichment in control T reg cells, respectively. Heat maps of gene expression levels within the leading edge (top 50 for A and B, and all for C) are shown. NES, normalized enrichment score; NOM p-val, nominal P values; FDR q-val, FDR q values generated from the GSEA algorithm. **(D and E)** Validation of expression changes in T reg–up signature genes (D) and cell cycle and antigen response-related genes (E) in Tcf1/Lef1-deficient T reg cells. T reg cells were sorted from old (≥24 wk) or young (6–8 wk) mice and analyzed by quantitative RT-PCR. The expression of each gene in T reg cells from the old *Foxp3*^{Cre} control mice was set at 1, and that in cells from other groups was normalized accordingly. Data are means ± SD from two independent experiments (n = 3 for each group). Statistical significance was determined by one way ANOVA, followed by Student's t test for indicated pairwise comparisons. ns, not statistically significant; *, P < 0.05; **, P < 0.01; ***, P < 0.001.

in Tcf1/Lef1-deficient T reg cells, the expression of *Gzmb* and *Prf1* remained substantially lower compared with bona fide effector CD8$^+$ T cells elicited by acute viral infection in vivo (Shan et al., 2017; Fig. S3 A). Therefore, Tcf1 and Lef1 prevent induction of the cytotoxic CD8$^+$ effector program in T reg cells, albeit loss of Tcf1/Lef1 may not reprogram the T reg cells to fully functional cytotoxic CD8$^+$ T cells. These data collectively suggest that Tcf1 and Lef1 are important for restraining T reg cells from excessive cycling and maintaining T reg cell identity. On the other hand, among gene sets enriched in control T reg cells, one prominent change is the "KEGG_WNT_SIGNALING_PATHWAY," showing diminished expression of 46 of 143 genes in the gene set in Tcf1/Lef1-deficient T reg cells (Fig. S3 B). This observation suggests that Tcf1 and Lef1 contribute to sustaining the responsiveness to Wnt ligands, consistent with a positive-feedback regulatory mechanism.

It has been shown that forced coexpression of Lef1 and Foxp3 induces expression of a subset of T reg signature genes in T conv CD4$^+$ T cells (Fu et al., 2012). By comparison of >100 microarray-based gene expression profiles of T reg and T conv CD4$^+$ T cells from multiple tissues, the Benoist and Mathis groups defined a set of T reg signature genes, which contains 295 over- and 137 underexpressed genes, called T reg–up and T reg–down genes, respectively (Fu et al., 2012). We used both gene sets in GSEA. This analysis revealed that the T reg–up gene set is positively enriched in control T reg cells, i.e., ∼25% (75 of 295 genes) showed diminished expression in Tcf1/Lef1-deficient T reg cells (Fig. 5 C). It should be noted, however, that the positive enrichment of T reg–up signature in control T reg cells was projected to be modest with GSEA, with an FDR of 0.132. By tracking the enrichment score generated by GSEA, another 25% (74 of 295) of T reg–up genes actually exhibited elevated expression in Tcf1/Lef1-deficient T reg cells, which was equivalent to a negative enrichment in control T reg cells (Fig. S3 C). Among the 74 genes up-regulated in Tcf1/Lef1-deficient T reg cells, 16 genes overlapped with cell cycle and antigen response genes found in Fig. 5 (A and B), including *Gzmb*.

Similarly, the T reg–down gene set was also positively enriched in control T reg cells as determined by GSEA, i.e., ∼30% (43 of 137 genes) were further diminished in expression in Tcf1/Lef1-deficient T reg cells (Fig. S3 D). This positive enrichment had an FDR of 0.131. Based on enrichment scores, ∼19% (26 of 137 genes) showed a tendency of negative enrichment in control T reg cells, i.e., up-regulated in expression in Tcf1/Lef1-deficient T reg cells (Fig. S3 D), and four genes including *Ccl5* and *Id2* overlapped with cell cycle and antigen response–related genes. Collectively, Tcf1 and Lef1 show a broader effect on balanced expression of T reg signature genes.

For in-depth molecular characterization of T reg signature genes, we focused on T reg–up signature genes that were down-regulated in Tcf1/Lef1-deficient T reg cells. For T reg–up and T reg–down signature genes that were up-regulated in Tcf1/Lef1-deficient T reg cells, because of their partial overlap with cell cycle and antigen response genes that exhibited extensive up-regulation in Tcf1/Lef1-deficient T reg cells, we characterized those genes collectively in the latter functional categories. By quantitative RT-PCR, we validated diminished expression of select T reg–up signature genes, including *Plga1*, *Trpm1*, *Gpr83*, *Mapk12*, *Lrig1*, *Ikzf4*, and *Izumo1r*, in T reg cells from *Foxp3*^{Cre}*Tcf7*$^{fl/fl}$*Lef1*$^{fl/fl}$ mice at ≥24 wk of age (referred to as old mice in Fig. 5 D). Among these, several genes have known roles in T reg cells. For example, *Ikzf4* encodes Eos transcription factor in the Ikaros family, which interacts with Foxp3 and is responsible for Foxp3-dependent gene silencing in T reg cells (Pan et al., 2009); *Gpr83* encodes G protein–coupled receptor 83, and its forced expression in T conv CD4$^+$ T cells was associated with Foxp3 induction and conferred the cells with suppressive activity (Hansen et al., 2006); and *Izumo1r* encodes folate receptor 4, which specifically marks anergic T conv CD4$^+$ T cells that have the capacity of differentiating into T reg cells (Kalekar et al., 2016).

To further exclude the possibility that the T reg–up signature expression changes were secondary to inflammatory responses, we used T reg cells from mice at 6–8 wk of age (referred to as young mice), which showed no detectable signs of aberrant T conv CD4$^+$ and CD8$^+$ T cell activation (Fig. S2, C and D). Although a few genes in T reg cells from young mice showed elevated (*Trpm1* and *Gpr83*) or modestly diminished (*Mapk12*, *Lirg1*, and *Izumo1r*) expression compared with those in old mice, all these genes were invariably reduced in expression in Tcf1/Lef1-deficient T reg cells from age-matched animals (Fig. 5 D).

In T reg cells from old Tcf1/Lef1-deficient mice, we also validated the increased expression in cell cycle–related genes including *Cdk1* and *Chek1* (encoding cyclin-dependent kinase 1 and check point kinase 1, respectively), antigen response genes such as *Kifl1*, *Brca1*, *Prdm1*, and *Id2*, and cytotoxicity genes associated with effector CD8$^+$ T cells including *Prf1* and *Gzmb* (Fig. 5 E). It is of interest to note that the increase in gene expression was also observed in Tcf1/Lef1-deficient T reg cells from young mice when they did not exhibit signs of inflammation (Fig. 5 E). These data corroborate that Tcf1 and Lef1 are intrinsically required for maintaining balanced expression of a subset of T reg signature genes and restraining T reg cells from excessive cycling and aberrant activation of the cytotoxic program–associated genes.

Identification of Tcf1 direct target genes in T reg cells

To define how Tcf1 and Lef1 contribute to transcriptomic regulation in T reg cells, we performed chromatin immunoprecipitation sequencing (ChIP-seq) of Tcf1 in WT T reg cells. We initially focused on Tcf1 because compared with Lef1, Tcf1 frequently exhibits a dominant regulatory effect in multiple T cell developmental stages and differentiation processes (Xue and Zhao, 2012), and an Tcf1 antibody made in-house performs more robustly in ChIP-seq analysis than commercially available Lef1 antibodies (Xing et al., 2016). Using a stringent setting of fourfold enrichment in WT T reg over Tcf1-deficient CD4$^+$ T cells, $P < 10^{-5}$ and FDR < 0.05, we identified 3,402 high-confidence Tcf1 binding peaks in T reg cells. Genome-wide Foxp3 binding sites in T reg cells have been previously defined in two independent studies (Samstein et al., 2012; Kitagawa et al., 2017). We adopted the approach used by the Benoist and Mathis groups (Kwon et al., 2017), i.e., selecting the top 5,000 Foxp3 sites with highest signals and replicated in both studies. Cross-comparison of global Tcf1 and Foxp3 binding peaks

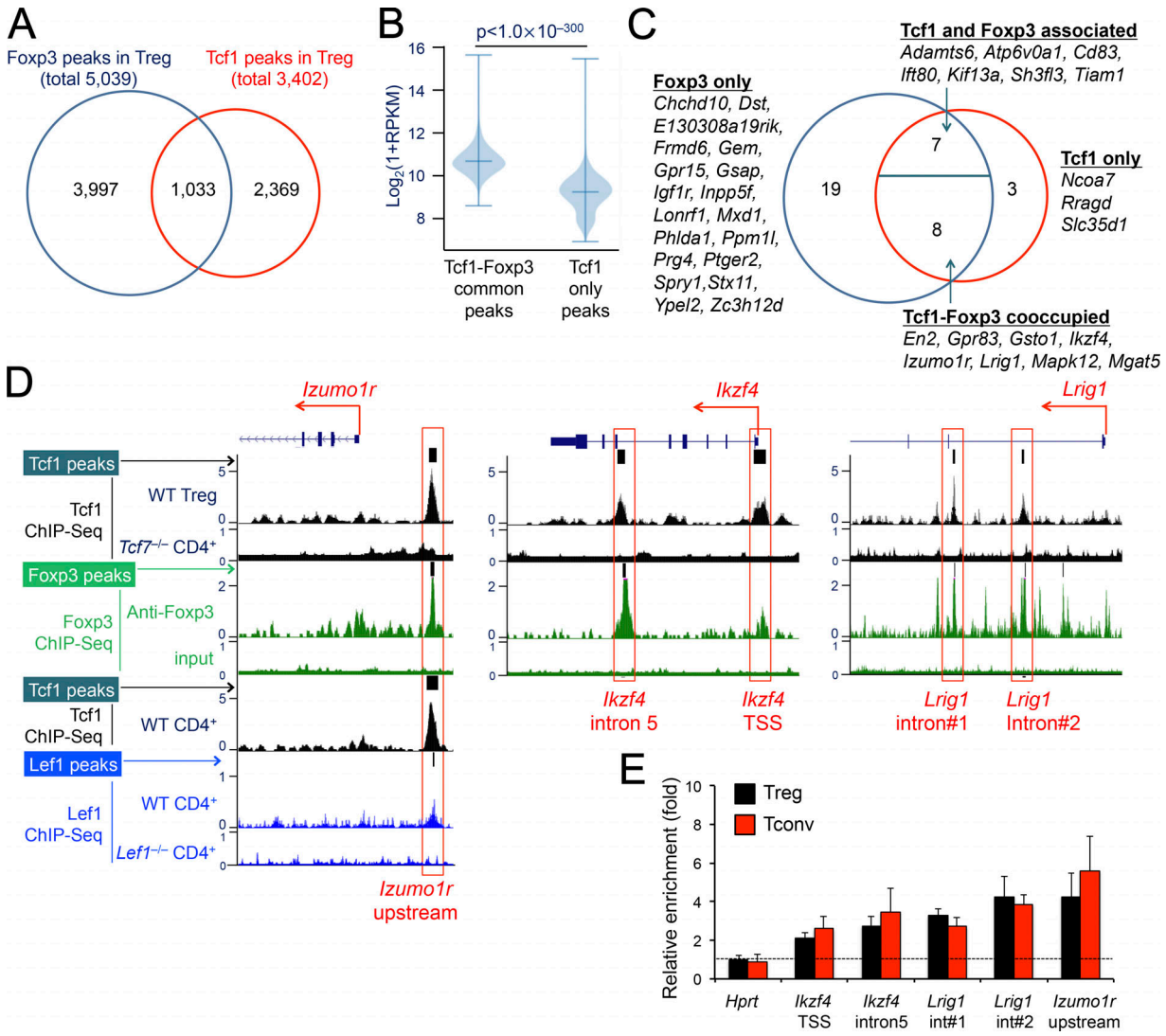

Figure 6. **Tcf1 and Foxp3 cooccupy at select T reg–up signature genes. (A)** Venn diagram showing distinct and overlapping Tcf1 and Foxp3 binding peaks in T reg cells. Tcf1 ChIP-seq was performed on WT T reg cells, and high-confidence Tcf1 binding peaks were compared with the top 5,039 reported Foxp3 peaks. Note that the value of 1,033 in the intersection denotes the number of Tcf1 peaks that overlapped with 1,042 of 5,039 Foxp3 peaks. **(B)** Violin plot showing Tcf1 binding strength (log_2(1+RPKM)) at regions cobound by Tcf1 and Foxp3 and those bound by Tcf1-only. The P value was determined using two-sided Mann–Whitney *U* test. **(C)** Tcf1 and Foxp3 binding events at the T reg–up signature genes. Tcf1 and Foxp3 binding peaks were identified within ±50 kb of the gene bodies of 75 T reg–up signature genes that showed diminished expression in Tcf1/Lef1-deficient T reg cells (as defined in Fig. 5 C, and further fractioned into groups harboring Tcf1-only, Foxp3-only, nonoverlapping Tcf1 and Foxp3 peaks [called Tcf1 and Foxp3 associated], and overlapping Tcf1 and Foxp3 peaks [called Tcf1-Foxp3 cooccupied]). The number and identity of genes in each group are shown. **(D)** Visualization of Tcf1, Lef1, and Foxp3 binding peaks at select T reg–up signature genes. Displayed on UCSC genome browser are ChIP-seq tracks at the *Izumo1r*, *Ikzf4*, and *Lrig1* gene loci in the following order: Tcf1 ChIP-seq tracks in WT T reg and Tcf1-deficient CD4+ T cells, Foxp3 ChIP-seq, and corresponding input track from Kitagawa et al. (2017). Tcf1 ChIP-seq tracks in WT CD4+ T cells and Lef1 ChIP-seq tracks in WT and Lef1-deficient CD4+ T cells are shown for *Izumo1r*, but not *Ikzf4* and *Lrig1* because the latter two genes did not harbor evident Lef1 binding peaks. MACS2-called Tcf1 and Lef1 peaks are shown as filled black bars on top of corresponding tracks; and for Foxp3 peaks, only the top 5,000 defined in Kwon et al. (2017) are marked with black bars. Y-axis denotes normalized read counts (fragments pile-up per million reads). The whole or partial gene structure and gene transcription orientations are also shown, with Tcf1 or Tcf1-Foxp3–cooccupied sites marked with red rectangles. **(E)** Tcf1 occupies the same sites in select T reg–up signature genes in T conv and T reg cells. T conv and T reg cells were sorted from *Foxp3*^{Cre} WT mice and analyzed with ChIP-qPCR for enriched binding of Tcf1 to the indicated genomic locations. Dotted horizontal line denotes a no-enrichment level at the *Hprt* locus. Data are means ± SD from two to three independent experiments with each sample measured in duplicate or triplicate. Although not marked for consideration of clarity, the enriched Tcf1 binding at each genomic location has $P < 0.001$ by Student's *t* test when compared with *Hprt* control in corresponding cell type.

showed that 1,033 locations were cooccupied by both factors (Fig. 6 A), consistent with a previous report that Foxp3 and Tcf1 may physically interact with each other in coimmunoprecipitation assays (van Loosdregt et al., 2013). Although Tcf1-only peaks and Tcf1-Foxp3 common peaks showed similar distribution, with ∼48% at the promoters (defined as ±1-kb regions flanking transcription start sites [TSSs]; Fig. S4 A), the Tcf1 binding strength to its target sites were significantly higher in

Tcf1-Foxp3 common peaks than in Tcf1-only peaks (Fig. 6 B), suggesting that cooccupancy by Foxp3 may have stabilized and/or enhanced Tcf1 binding. De novo motif analysis revealed that Tcf1-Foxp3 common peaks were indeed enriched in Tcf/Lef motif, as well as Ets and Runx motifs (Fig. S4 B). Analysis with the find individual motif occurrence (FIMO) algorithm revealed 20–25% occurrence of Tcf/Lef motif in Tcf1 peaks and ∼10% of Foxp3 motif in Foxp3 peaks, with the highest occurrence of both motifs in Tcf1-Foxp3 common peaks (Fig. S4 C). These analyses suggest that Tcf1 and Foxp3 may cooperate functionally in T reg cells.

To further define molecular connection of Tcf1 with its key target genes in T reg cells, we examined Tcf1 and Foxp3 binding events in genes that are differentially expressed in Tcf1/Lef1-deficient T regs and are associated with key T reg functions as defined by GSEA. We focused on −50 kb to +50 kb genomic regions that flanked the gene body, a strategy that was used previously to characterize Foxp3 targets in T reg cells (Kwon et al., 2017). Among the 75 T reg–up signature genes that showed diminished expression in Tcf1/Lef1-deficient T reg cells (Fig. 5 C), 17 genes contained Tcf1 binding peaks (Fig. 6 C). Whereas three genes had Tcf1 binding peaks only and six genes contained Tcf1 and Foxp3 peaks at different locations, eight genes harbored Tcf1 and Foxp3 cooccupied sites (Fig. 6 C). For example, Tcf1 and Foxp3 showed cobinding to an upstream region of *Izumo1r*, an intron 5 region in *Ikzf4* (encoding EOS), and intronic regions of *Lrig1*, whereas Tcf1 bound to *Ikzf4* TSS as well (Fig. 6 D). The direct association of Tcf1 with these genomic locations was also validated by ChIP-PCR in T reg cells (Fig. 6 E), highlighting a direct regulatory role of Tcf1 in a subset of T reg–up signature genes. In addition, we noted that Tcf1 bound to the same genomic locations of these T reg–up signature gene loci in T conv CD4$^+$ T cells as well (Fig. 6 E). In line with the notion that Foxp3 exploits preexisting enhancers to confer T reg–specific gene regulations (Samstein et al., 2012), our data suggest that at least a portion of Tcf1-binding sites in T conv CD4$^+$ T cell genome may be used by Foxp3 to establish T reg cell identity.

We also examined the 203 of 315 genes in the "GOLDRATH_ANTIGEN_RESPONSE" gene set and the 185 of 377 genes in the "REACTOME_CELL_CYCLE" gene set that showed increased expression in Tcf1/Lef1-deficient T reg cells (Fig. 5 B and Fig. 5 A, respectively). 27 "antigen response" genes and 30 "cell cycle" genes had Tcf1 binding peaks within the ±50-kb regions flanking their gene bodies (Fig. 7, A and B). Of these Tcf1-associated genes, 13 antigen response genes and 8 cell cycle genes contained Tcf1 and Foxp3 cooccupied sites (Fig. 7, A and B). For example, Tcf1 and Foxp3 cobound to the TSSs of *Brca1* and *Kif11*, an upstream region of *Ifng* (encoding IFN-γ), and upstream and intronic regions of *Prdm1* (Fig. 7 C). Direct Tcf1 binding to these key genomic sites was also validated by ChIP-PCR in T reg as well as T conv CD4$^+$ T cells (Fig. 7 D). These data further corroborate an intrinsic requirement for Tcf1 in preventing aberrant activation of cytotoxic program–associated genes in T reg cells and restrain T regs from excessive cycling. To further substantiate this point, we used CRISPR/Cas9 technology to target the *Prdm1* upstream region that was ∼24 kbp from its TSS. As highlighted in Fig. 7 C (lower left panel), this region was bound by both Tcf1 and Lef1, contained several Tcf/Lef binding motifs (Fig. S4 D), and was also associated with a discernible Foxp3 peak (albeit not among the top 5,000 Foxp3 binding sites). Deletion of the −24 kb *Prdm1* region in mouse germline was sequence-verified (Fig. S4 D). In mice that were homozygous for the deletion mutation (called −24-kb *Prdm1*$^{m/m}$), *Prdm1* expression was elevated by approximately twofold in T reg cells, similar to its expression changes observed in Tcf1/Lef1-deficient T reg cells (Fig. 7 E, compare with Fig. 5 E). Importantly, the expression of *Prf1* (another cytotoxic effector gene) and *Ikzf4* (a T reg–up signature gene), which were 17 Mbp and 84 Mbp away from *Prdm1* on the same chromosome 10, respectively, was not affected in −24-kb *Prdm1*$^{m/m}$ T reg cells (Fig. 7 E). These findings exemplify the direct contribution of Tcf1 and Lef1 to suppressing cytotoxic programs in T reg cells and hence protecting T reg cell identity.

Functional redundancy between Tcf1 and Lef1

A single Tcf/Lef orthologue is expressed in invertebrates, such as pangolin in *Drosophila* and POP-1 in *Caenorhabditis elegans* (Arce et al., 2006). Four Tcf/Lef genes in the HMG subfamily are acquired in higher organisms, with distinct and overlapping functions (Arce et al., 2006). Tcf1 and Lef1 are the only two factors that are expressed in T cells, and they exhibit functional redundancy in multiple biological processes, including maturation of CD4$^-$CD8$^-$ double-negative thymocytes to the CD4$^+$CD8$^+$ double-positive stage (Okamura et al., 1998; Yu et al., 2012), CD4$^+$ lineage choice of postselect double-positive thymocytes (Steinke et al., 2014), establishment of CD8$^+$ T cell identity (Xing et al., 2016), differentiation of CD4$^+$ T cells into Tfh cells (Choi et al., 2015), and generation of memory precursor and memory cells after CD8$^+$ T cell activation elicited by acute infection (Zhou et al., 2010; Zhou and Xue, 2012). It is frequently observed that ablation of Lef1 alone shows either no detectable or very modest impact on all the biological processes described above, while loss of Tcf1 alone results in more discernable defects. Only when both factors are ablated, are more profound impacts observed. This was true for their roles in T reg cells as described in detail above. The lack of defects in Lef1-deficient T cells is generally ascribed to the almost complete compensatory function by Tcf1. It remains unclear, however, whether Lef1 has its own unique target genes in T cells.

We then performed Tcf1 and Lef1 ChIP-seq in T conv CD4$^+$ T cells. Although the Lef1 antibody performed less robustly in ChIP-seq studies compared with the Tcf1 antibody, we detected 1,990 unambiguous Lef1 peaks, whereas 4,505 Tcf1 peaks were detected (Fig. 8 A). About one-third of Lef1 peaks overlapped with Tcf1 peaks, and Tcf1 and Lef1 binding strength were stronger at the Tcf1-Lef1 common sites than that at Tcf1-specific or Lef1-specific sites, respectively (Fig. 8 B). These observations were consistent with a recent report on Tcf1 and Lef1 binding peaks in double-positive thymocytes (Emmanuel et al., 2018), and both studies identified genomic locations that were bound by Lef1 but not Tcf1. Because Tcf1 frequently bound to key T reg gene loci in both T conv CD4$^+$ and T reg cells as validated in Figs. 6 E and 7 D, and lower Lef1 expression in T reg cells, as shown in Fig. 1 A, further hindered Lef1 ChIP-seq in T reg cells per se with

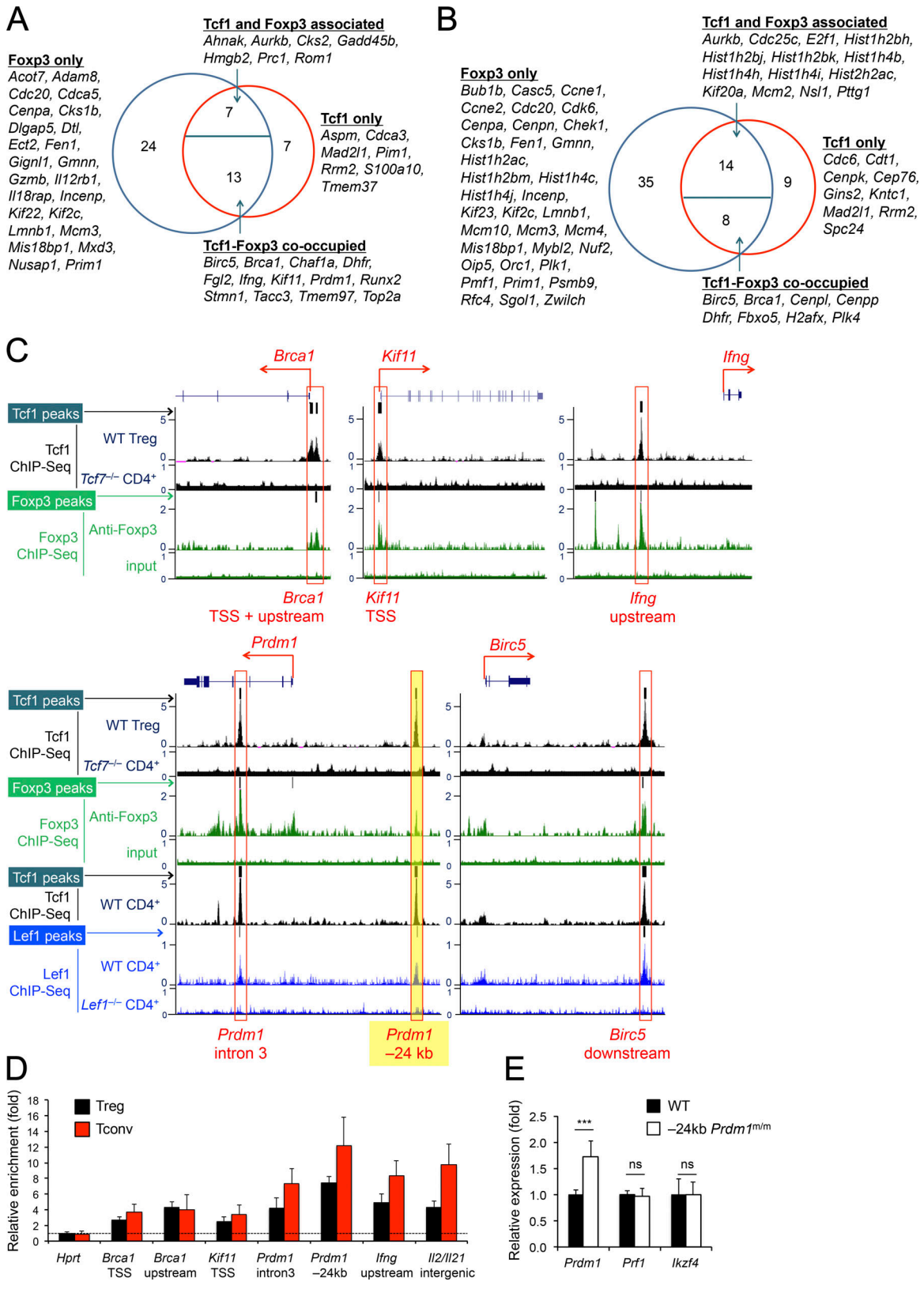

Figure 7. **Tcf1 and Foxp3 cooccupy at select genes regulating cell cycle and antigen responses. (A and B)** Tcf1 and Foxp3 binding events at genes regulating cell cycle and antigen responses. Tcf1 and Foxp3 binding peaks were identified within ±50 kb of the gene bodies of 203 antigen response genes (A) and 185 cell cycle genes (B) that showed increased expression in Tcf1/Lef1-deficient T reg cells (as defined in Fig. 5 B and Fig. 5 A, respectively). These peaks were further fractioned into groups harboring Tcf1-only, Foxp3-only, Tcf1 and Foxp3 associated, and Tcf1-Foxp3 cooccupied peaks. The number and identity of genes in each group are shown. **(C)** Visualization of Tcf1, Lef1, and Foxp3 binding peaks at select cell cycle or antigen response genes. Displayed on UCSC genome browser are ChIP-seq tracks at the *Brca1*, *Kif11*, *Ifng*, *Prdm1*, and *Birc5* gene loci, in the same format as in Fig. 6 D. Lef1 ChIP-seq tracks are not shown for

the three genes in top panels because they did not harbor evident Lef1 binding peaks. Highlighted in yellow at the *Prdm1* locus is the −24-kb upstream region that was targeted by CRISPR/Cas9 in Fig. 7 E. **(D)** Tcf1 occupies the same sites in select genes regulating cell cycle and antigen responses in T conv and T reg cells. T conv and T reg cells were analyzed with ChIP-qPCR for enriched binding of Tcf1 to the indicated genomic locations. Dotted horizontal line denotes a no-enrichment level at the *Hprt* locus. Data are means ± SD from two to three independent experiments with each sample measured in duplicate or triplicate. The enriched Tcf1 binding at each genomic location has $P < 0.001$ by Student's *t* test when compared with *Hprt* control in corresponding cell type (not marked). **(E)** The Tcf1/Lef1-bound −24-kb region contributes to *Prdm1* repression in T reg cells. TCRβ$^+$CD4$^+$CD25$^+$ T reg cells were sorted from −24-kb *Prdm1*$^{m/m}$ or WT littermates (6–8 wk) and analyzed for expression of *Prdm1* and two other genes on the same chromosome 10 by RT-PCR. The expression of each gene in WT T reg cells was set at 1, and that in mutant cells was normalized accordingly. Data are means ± SD from two experiments ($n = 3$ for each group). ns, not statistically significant; ***, $P < 0.001$ by Student's *t* test.

a less robust antibody, we used Lef1 binding events in T conv CD4$^+$ cells to infer Lef1 target genes in T reg cells. Such analyses suggest that Lef1 contributed to proper expression of T reg-up signature genes (such as *Izumo1r*; Fig. 6 D), and restrained expression of CD8$^+$ effector- and cell cycle–associated genes (such as *Prdm1* and *Birc5*; Fig. 7, C and E), by occupying the same sites that Tcf1 and Foxp3 bound together, or the same sites that Tcf1 bound without involving Foxp3 (Fig. 8, C and D). In addition, Lef1 may also bind to genes in these functional categories, together with Foxp3 (such as *Bub1b*) or by itself (such as *Ccr2*; Fig. 8 E), where we did note that Lef1 peaks were weaker compared with those at Tcf1-Lef1–common sites, consistent with the global analysis (Fig. 8 B).

Based on functional and molecular analyses in this work and previous published data, we propose an updated model to explain the redundancy between Tcf1 and Lef1 (Fig. 8 F). In spite of their highly conserved DNA binding domain, Tcf1 and Lef1 have both common and unique binding sites in a T cell genome. The binding locations and their flanking sequences, coupled with distinctive cofactors that are directly or indirectly recruited by Tcf1 or Lef1, form distinctive features of the binding sites. Some sites can accommodate both Tcf1 and Lef1 proteins and function as Tcf1-Lef1 common sites, whereas other sites favor binding by one factor but not the other and thus function as Tcf1- or Lef1-unique sites. Tcf1 binds to a larger number of genomic locations besides the Tcf1-Lef1 common sites, with more potent binding strength; as a result, loss of Tcf1 cannot be fully compensated by the expression of Lef1 and leads to discernible defects. On the other hand, with a caveat of reagent quality in mind, Lef1 binds to fewer sites with less potent binding strength. These Lef1-unique binding events, therefore, do not amount to substantial biological changes in T cells when Lef1 alone is genetically ablated, but remain functionally critical in the context of Tcf1 deficiency. This model may help explain the differences in autoimmune phenotypes in mice where Tcf1 or Lef1 was ablated alone or in combination in T reg cells, and may be applicable to other T cell biological processes as well.

Functional interplay between Tcf1/Lef1 and Foxp3

It is generally accepted that Foxp3 exploits existing enhancer elements in T reg precursor cells to establish appropriate T reg transcriptome (Samstein et al., 2012). Because Tcf1 is shown to physically interact with Foxp3 (van Loosdregt et al., 2013) and Tcf1/Lef1 and Foxp3 showed cooccupancy at a portion of their target sites, we next asked if Tcf1 and Lef1 are responsible for recruitment of Foxp3 to its target sites. We tested this at select Tcf1-Foxp3 cooccupied sites, which were associated with genes that were differentially expressed in Tcf1/Lef1-deficient T reg cells, as characterized in Figs. 5, 6, and 7. As measured by ChIP coupled with qPCR, Foxp3 exhibited no enriched binding to *Gmpr*, a negative control site, and similar enriched binding at the *Ctla4* TSS, a positive control (Zheng, 2011) in control and Tcf1/Lef1-deficient T reg cells (Fig. S5 A). Consistent with the reported ChIP-seq data (Samstein et al., 2012; Kitagawa et al., 2017), Foxp3 exhibited enriched binding in WT T reg cells to *Ikzf4* and *Lrig1* introns, and an upstream region of *Izumo1r* (refer to Fig. 6 D), and to upstream regions of *Brca1*, *Ifng*, and *Prdm1* (refer to Fig. 7 C); importantly, the Foxp3 binding at these genomic locations was not significantly different in Tcf1/Lef1-deficient T reg cells (Fig. S5 A). These data suggest that the recruitment of Foxp3 to the Tcf1-Foxp3 cooccupied sites may not be dependent on Tcf1 and/or Lef1 per se. As shown in Fig. 5 (D and E), however, these Tcf1-Foxp3 cobound genes were either down-regulated (for *Ikzf4*, *Lrig1*, and *Izumo1r*) or up-regulated (for *Brca1*, *Ifng*, and *Prdm1*) in Tcf1/Lef1-deficient T reg cells, indicating that the Tcf1/Lef1 binding events are biologically consequential (as also exemplified in Fig. 7 E). Foxp3 is shown to form multiprotein complexes of 400–800 kD or larger (Rudra et al., 2012). Tcf1 and Lef1 may function as critical components in a portion of Foxp3 complexes and contribute to Foxp3 regulatory output therein, even if they do not function as the primary Foxp3 recruiters.

As observed in the chronic colitis model, maintenance of Foxp3 expression in Tcf1/Lef1-deficient T reg cells was impaired (Fig. 3, H and I), suggesting Tcf1 and Lef1 may contribute to positive regulation of Foxp3 when T reg cells are under proliferative stress in a lymphopenic environment. Foxp3 binds to the conserved noncoding sequence (CNS) 2 element in the first intron *Foxp3* to positively sustain its own expression (Zheng et al., 2010; Kitagawa et al., 2017). Whereas neither Tcf1 nor Lef1 bound to the known CNS elements, Tcf1 did bind to an element at ∼38 kb downstream of Foxp3 TSS (Fig. S5 B), although the biological significance of this binding requires more investigation. Tcf1 and Lef1 may also contribute to *Foxp3* regulation via indirect mechanisms through T reg–up signatures such as Eos.

Previously it was reported that Tcf1 and Foxp3 were both associated with *Il2* promoter when overexpressed, and gain-of-function analysis by stimulating Wnt pathway caused increased IL-2 production in both human and mouse T reg cells (van Loosdregt et al., 2013). In our unbiased mapping of Tcf1 binding in T regs, we found a sole Tcf1 and Foxp3 cooccupied site in an intergenic region between *Il2* and *Il21* (Fig. S5 C) and validated Tcf1 binding to this site in T reg and T conv CD4$^+$ cells (Fig. 7 D). Neither gene was differentially expressed in Tcf1/Lef1-deficient

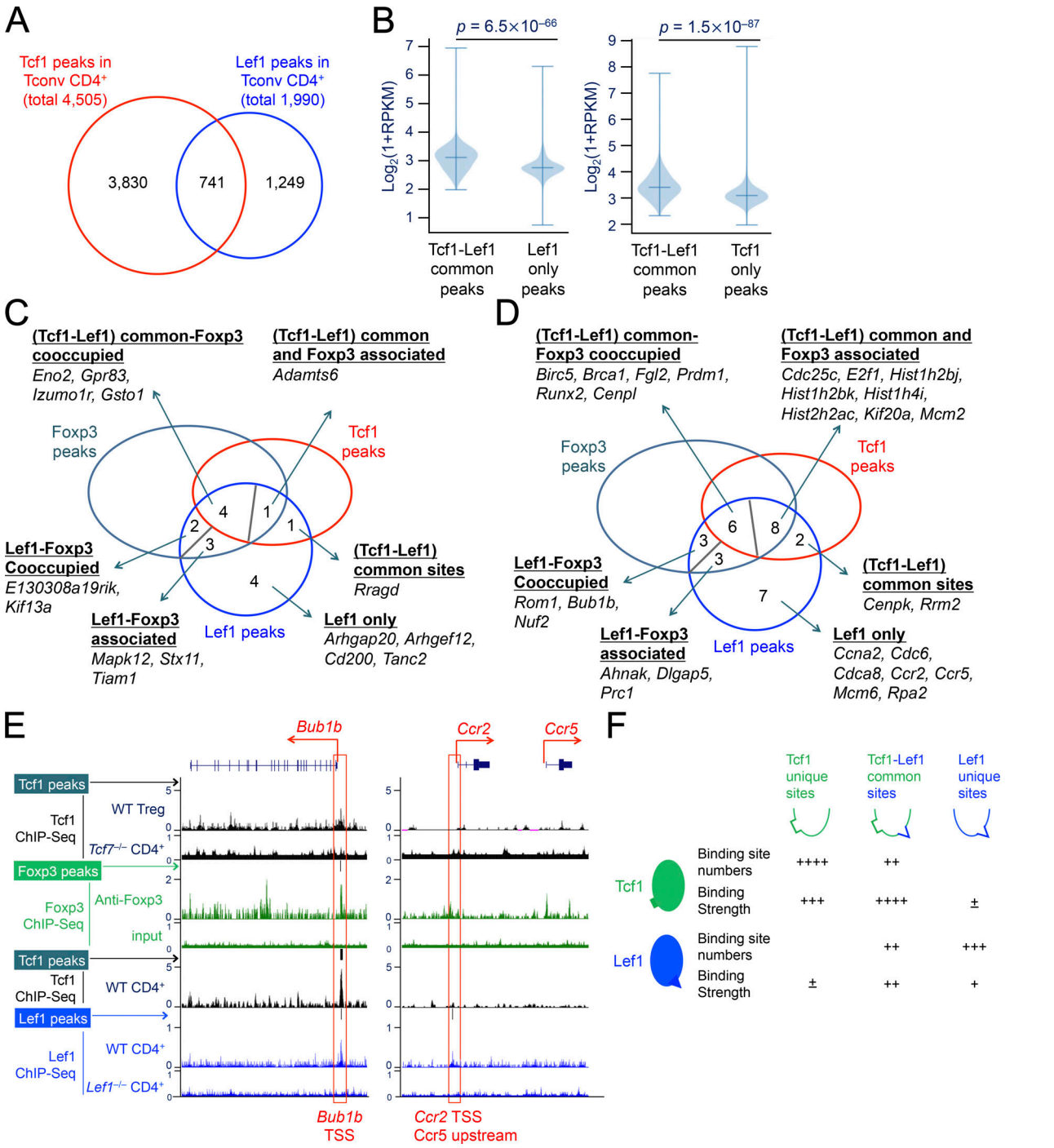

Figure 8. **Tcf1 and Lef1 share common and distinct targets in T cell genome. (A)** Venn diagram showing distinct and overlapping Tcf1 and Lef1 binding peaks in T conv CD4+ T cells. The value of 741 in the intersection denotes the number of Lef1 peaks that overlapped with 675 of 4,505 Tcf1 peaks. **(B)** Violin plots showing Lef1 binding strength (log_2(1+RPKM)) in Tcf1-Lef1 common peaks and Lef1-only peaks (left), and Tcf1 binding strength (log_2(1+RPKM)) in Tcf1-Lef1 common peaks and Tcf1-only peaks. The P values were determined using two-sided Mann–Whitney *U* test. **(C and D)** Lef1 binding events at T reg–up signature genes (C) and cell cycle/antigen response genes (D). Lef1 peaks were identified within ±50 kb of the gene bodies defined in Figs. 6 C and 7 (A and B). Tcf1-Lef1 common or Lef1-only sites were further fractioned into groups where these sites showed cooccupancy with Foxp3, nonoverlapping but associated with Foxp3 peaks, or no connection with Foxp3 peaks. The number and identity of genes in each group are shown. **(E)** Visualization of Tcf1, Lef1, and Foxp3 binding peaks at select gene loci. Displayed on UCSC genome browser are ChIP-seq tracks at the *Bub1b*, *Ccr2*, and *Ccr5* gene loci. Refer to Fig. 6 D for Lef1 binding peaks at *Izumo1r* and Fig. 7 C for Lef1 binding peaks at *Prdm1* and *Birc5* loci. **(F)** Proposed model to explain Tcf1 and Lef1 functional redundancy in T cells. See text for details.

T regs based on our RNA-seq analysis. On protein levels, however, Tcf1/Lef1-deficient T regs showed modest reduction in IL-2 production in response to TCR stimulation (Fig. S5 D). Our loss-of-function analysis is consistent with the notion that Tcf1 and Foxp3 may act together to regulate IL-2 levels in T reg cells, albeit the underlying molecular details may differ.

Discussion

In this study, by specific and conditional targeting of Tcf1 and Lef1 in T reg cells, we demonstrated that these two factors are essential for sustaining the T reg suppressive functions and maintaining immune homeostasis. Although Tcf1 and Lef1 expression was reported to be underexpressed in T reg compared with T conv CD4$^+$ T cells, and dubbed among T reg–low signature genes (Hill et al., 2007; Fu et al., 2012; Barra et al., 2015), our study revealed that the lower expression of Tcf1 and Lef1 remained critical for T reg cells to be effective immune repressors. Defining T reg signature genes has been a useful approach to dissect the regulatory output by Foxp3 and other key T reg transcription regulators. However, excessive expression of T reg–up signature genes or inadequate expression of T reg–down signature genes does not appear to be always compatible with proper functionality expected from normal T reg cells. It seems reasonable to deduce that balanced expression of T reg signature genes at appropriate levels remain critical for sustaining the immunosuppressive functions of T reg cells. The intrinsic requirement for a T reg signature gene or gene family necessitates careful, case-by-case investigation.

Whereas Tcf1/Lef1-deficient T reg cells did not exhibit functional changes when tested using in vitro suppression assay, they were much less effective in preventing inflammation in vivo in both acute and chronic colitis models than WT T reg cells. It was reported that Tcf1-null T reg cells derived from germline-targeted mice showed stronger suppressive activity in vitro (van Loosdregt et al., 2013). This difference may lie with the timing of Tcf1 deletion, because Tcf1 and Lef1 are now known to critically regulate several critical steps during T cell development, including T lineage specification, transition from double-negative to double-positive stage, and CD4$^+$ T cell lineage choice (Germar et al., 2011; Weber et al., 2011; Yu et al., 2012; Steinke et al., 2014). T cells generated from Tcf1-deficient hematopoietic progenitors may have altered chromatin configuration, and the resulting Tcf1-deficient T reg cells inheriting such alterations may behave differently.

Like many other transcription factors, Foxp3 can function as either transcription activator or repressor, which is considered to depend on the interacting factors in different gene context (Rudra et al., 2012; Kwon et al., 2017). By retrovirus-mediated gene delivery that required priming TCRs in T conv cells, it was previously suggested that Lef1, when coexpressed with Foxp3, could help establish at least a portion of T reg signature genes (Fu et al., 2012). Our analysis of T reg cells, WT or Tcf1/Lef1-targeted, did not involve TCR stimulation and focused on their homeostatic state in vivo. Through careful analyses of the transcriptomic changes upon loss of Tcf1 and Lef1 and cross-comparison of genome-wide Tcf1 and Foxp3 binding maps in T reg cell genome, we defined a more precise subset of T reg–up signature that is controlled by Tcf1 and Lef1. Several genes with known functions in T reg cells (such as *Ikzf4*) all harbored Tcf1 and Foxp3 cooccupied sites. Although Tcf1 and Lef1 are not necessarily required for direct recruitment of Foxp3 to its target sites, their cooperativity with Foxp3 might be rather on the functional aspect, that is, Tcf1 and Lef1 act as important components in Foxp3-centric multiprotein complexes and potentiate its target gene activation or repression.

One unexpected transcriptomic change in Tcf1/Lef1-deficient T reg cells was the induction of genes associated with the cytotoxic programs in effector CD8$^+$ T cells, including up-regulation of the cytotoxic molecules granzyme B and perforin, cytokine IFN-γ, and transcriptional regulators Blimp1 and Id2. It has been shown that T reg cells express little granzyme B or perforin at a resting state, but can be potently up-regulated upon activation in vitro (Zhao et al., 2006). Our data indicate that the suppression of these cytotoxic CD8$^+$ effector genes requires Tcf1 and Lef1, as exemplified by a repressive regulatory function of a Tcf1/Lef1-bound upstream region at the *Prdm1* locus. In the context of CD8$^+$ T cell development, Tcf1 and Lef1 are required not only for silencing CD4$^+$ lineage-associated genes such as *Cd4* and *Cd40lg*, but also for restraining aberrant induction of Blimp1, granzyme B, and perforin in naive CD8$^+$ T cells before TCR priming (Xing et al., 2016). Upon stimulation by their cognate antigens, naive CD8$^+$ T cells are activated and differentiate into effector CD8$^+$ T cells that are equipped with cytotoxic molecules and cytokines. This process depends on a number of transcription factors including Runx3; however, down-regulation of Tcf1 appears to be a necessary molecular event to facilitate optimal induction of the cytotoxic program (Shan et al., 2017). Therefore, Tcf1/Lef1-mediated repression of CD8$^+$ cytotoxic program genes may represent a conserved regulatory circuit that is used in multiple T cell subsets at different stages of development and immune responses.

Tcf1 and Lef1 are known to act downstream of the Wnt signaling pathway, activation of which leads to stabilization of the β-catenin coactivator. Indeed, loss of Tcf1 and Lef1 in T reg cells resulted in diminished expression of several molecules in the Wnt pathway, including the frizzled receptors and Lrp coreceptor, suggesting a self-enforcing regulatory circuitry. However, existing studies have reported contradicting observations upon stimulation of the Wnt-β-catenin pathway. Using forced expression of a stabilized form of β-catenin by retroviral transduction enhanced T reg cell survival and conferred better protective capacity to T reg cells in a colitis model (Ding et al., 2008). Recent studies showed, however, that strong or persistent Wnt stimulation inhibited the T reg suppressive function (van Loosdregt et al., 2013; Sumida et al., 2018). Similar discrepant observations were also made in studies of hematopoietic stem cells and T cell development (Xie et al., 2005; Guo et al., 2007; Luis et al., 2011). Nonetheless, a recurring theme appears to be that the dosage of Wnt stimulation and corresponding β-catenin protein levels are the critical determinants, with lower Wnt/β-catenin showing beneficial effects and excessively strong/persistent activation of this pathway being detrimental (Luis et al., 2011). In line with this view, the lower expression of

Tcf1 and Lef1 in T reg compared with T conv CD4+ T cells might reflect a physiological need to avoid hyperactivation of Wnt pathway and ensuing inhibition of T reg cell functions. On the other hand, the regulatory roles of Tcf1 and Lef1 are not solely dependent on β-catenin. In addition to Foxp3, Tcf1 and Lef1 interact with the TLE corepressors (Xing et al., 2018), histone methyltransferase Ezh2 (Li et al., 2018), and several other transcription factors such as Runx3 and Gata3 (Hossain et al., 2008; Steinke et al., 2014). Furthermore, Tcf1 and Lef1 are recently shown to harbor intrinsic histone deacetylase activity, which is required for establishing CD8+ T cell identity (Xing et al., 2016). It merits further investigation to fully dissect transcriptional and epigenetic regulator composition in Foxp3-dependent and -independent complexes that establish T reg cell identity. Nonetheless, our studies revealed a critical contribution of Tcf1 and Lef1 to sustaining T reg suppressive function and defined important downstream targets that are controlled by the Tcf/Lef module and its functional cooperation with Foxp3.

Materials and methods

Mice

Tcf7- and *Lef1*-floxed mice were previously generated, which were backcrossed to C57BL/6 for at least 10 generations (Yu et al., 2012; Steinke et al., 2014), and *Tbx21*-floxed mice and *Foxp3*^{Cre} mice were from The Jackson Laboratory (stock no. 022741 and 016959, respectively; Intlekofer et al., 2005; Rubtsov et al., 2008). Note that *Foxp3*^{Cre} mice refer to *Foxp3*-Cre$^{+/+}$ female or *Foxp3*-Cre$^{+/y}$ male mice throughout this article. *Foxp3*^{Cre} control mice include the following genotypes: *Foxp3*^{Cre}*Tcf7*$^{+/+}$*Lef1*$^{+/+}$, *Foxp3*^{Cre}*Tcf7*$^{fl/+}$*Lef1*$^{+/+}$, *Foxp3*^{Cre}*Tcf7*$^{+/+}$*Lef1*$^{fl/+}$, and *Foxp3*^{Cre}*Tcf7*$^{fl/+}$*Lef1*$^{fl/+}$, and all were phenotypically similar. All animals were analyzed at 5–30 wk of age, and both sexes were included without randomization or blinding. All mouse experiments were performed under protocols approved by the Institutional Animal Use and Care Committee of the University of Iowa.

Targeting the −24-kbp region in *Prdm1* gene locus using CRISPR/Cas9

Chemically modified CRISPR/Cas9 RNAs (crRNAs; 5′-CGCTGT CGTTCATGTTGTGT-3′ and 5′-TGGCTGATCAACAGGCTACA-3′) and transactivating crRNAs (tracrRNAs) were purchased from Integrated DNA Technologies (IDT) and used to target the −24-kbp upstream region in the *Prdm1* gene (Fig. S4 D). Individual cr:tracrRNA:Cas9 ribonucleoprotein complexes were made by combining cr:tracrRNA (50 ng/µl) with Cas9 nuclease protein (IDT; 200 ng/µl) and electroporated into pronuclear-stage embryos collected from C57BL/6J mice (The Jackson Laboratory), followed by implantation into pseudo-pregnant Hsc:ICR (CD-1; Envigo) females. Offspring born to the foster mothers were genotyped, and deletion of the entire region between the two crRNAs in the founders was verified by DNA sequencing.

Flow cytometry and cell sorting

A single-cell suspension was prepared from thymus, spleen, or lymph nodes and then surface-stained. All fluorochrome-conjugated antibodies were from eBiosciences unless indicated otherwise. The antibodies and their clone numbers are CD45.2 (104), CD45.1 (A20), CD4 (RM4-5), CD8α (53-6.7), TCRβ (H57-597), CD25 (PC61.5), GITR (DTA-1), CD62L (MEL-14), CD44 (IM7), CD28 (37.51), Nrp1 (3SS304M), CTLA4 (UC10-4B9), IFN-γ (XMG1.2), IL-17A (eBio17B7), CXCR3 (CXCR3-173), and IL-2 (JES6-5H3). For intracellular staining, anti-Ki-67 (B56; BD Biosciences), anti-human Granzyme B (GB12) and corresponding isotype control (mouse IgG1; Thermo Fisher Scientific/Invitrogen), anti-mouse Tcf1 (CD63D9), anti-mouse Lef1 (C12A5) and corresponding isotype control (rabbit mAb IgG DA1E; Cell Signaling Technology), anti-mouse Helios (22F6), anti-mouse Foxp3 (FJK-16s), and anti-mouse T-bet (4B10) were used. For intracellular detection of cytokine production, the cells from spleen or lymph nodes were stimulated with PMA (50 ng/ml) and ionomycin (1 µg/ml) in the presence of monensin and Brefeldin A for 5 h before fixation and permeabilization. Data were collected on FACSVerse (BD Biosciences) and analyzed with FlowJo software (version X; TreeStar). For cell sorting, surface-stained cells were sorted on BD FACSAria II or FACSAria Fusion cell sorter.

Colitis models

For induction of acute colitis with DSS, *Foxp3*^{Cre} control and *Foxp3*^{Cre}*Tcf7*$^{fl/fl}$*Lef1*$^{fl/fl}$ mice were used at 8–12 wk of age before autoimmune phenotypes developed. In preliminary studies, the concentrations of DSS were titrated so that *Foxp3*^{Cre} control mice had delayed onset of colonal inflammation, allowing detection of accelerated disease development in *Foxp3*^{Cre}*Tcf7*$^{fl/fl}$*Lef1*$^{fl/fl}$ mice. The mice were given 1.75% DSS in drinking water for 8 d, and the body weight was monitored daily. On day 9, mice were sacrificed and lymphoid organs harvested for analysis of CD8+ and T conv CD4+ T cell activation and IFN-γ production.

For induction of chronic colitis by T conv CD4+ T cells, CD45.1+ CD45RB^{hi}CD25−TCRβ+ naive CD4+ T cells were sort-purified from B6.SJL mice and adoptively transferred into *Rag1*$^{-/-}$ mice at 0.5 × 10^6 cells per mouse. To test the capacity of T reg cells in suppressing the naive T cell–induced colitis, TCRβ+CD4+YFP+ T reg cells were sort-purified from *Foxp3*^{Cre} control or *Foxp3*^{Cre}*Tcf7*$^{fl/fl}$*Lef1*$^{fl/fl}$ mice at 8–12 wk of age and cotransferred with naive CD4+ T cells into *Rag1*$^{-/-}$ mice at 0.25 × 10^6 cells per mouse. The *Rag1*$^{-/-}$ recipients were monitored weekly for body weight and signs of colitis. 6–8 wk later, colons were harvested for histological analysis, and mesenteric lymph nodes were used for phenotypic characterization of donor-derived lymphocytes.

Histology and disease scores

Tissues were collected at necropsy and placed in 10% neutral buffered formalin. After 5–7 d, the tissues were routinely processed, paraffin-embedded, sectioned (~4 µm), and stained by hematoxylin and eosin. Tissues were examined by a pathologist by following the principles of reproducible scoring methods (Meyerholz and Beck, 2018). The pathologist (D.K. Meyerholz) was masked to group assignments by the postexamination method (Meyerholz et al., 2018), so as to be effective and unbiased in scoring tissues from these models. Inflammatory infiltrates were generally scored for each organ using an ordinal

scoring system: 0, normal; 1, mild, uncommon focal infiltrates by scattered leukocytes; 2, moderate, multifocal infiltrates that start to form discrete aggregates; and 3, extensive, common infiltrates that coalesce into sheets of leukocytes.

In vitro suppression assay

Splenic TCRβ$^+$CD4$^+$YFP$^+$ T reg cells were sorted from *Foxp3*^{Cre} control and *Foxp3*^{Cre}*Tcf7*$^{fl/fl}$*Lef1*$^{fl/fl}$ mice at 8–12 wk of age. CD4$^+$CD25$^-$ naive T cells were enriched from B6.SJL congenic mice and labeled with Cell Trace Violet (CTV; Thermo Fisher Scientific/Molecular Probes) as responder cells. Total splenocytes were irradiated at 2,000 rad as antigen-presenting cells (APCs). In each well of a 96-well plate, APCs and CTV-labeled responder cells were seeded at 2 × 10^5 and 0.5 × 10^5 cells/well, respectively; and T reg cells were added at 0:4, 1:4, 2:4, or 4:4 ratios to responder cells and cultured for 60 h in the presence of soluble anti-CD3 mAb at 1 µg/ml. The division of CD45.1$^+$ responder cells was determined by detecting CTV dilution on a FACSVerse cell analyzer.

RNA-seq and data analysis

Splenic Thy1.2$^+$CD4$^+$YFP$^+$ T reg cells were sorted from male *Foxp3*^{Cre} control and *Foxp3*^{Cre}*Tcf7*$^{fl/fl}$*Lef1*$^{fl/fl}$ mice at 16 wk of age. Two biological replicates were obtained for each genotype and used for RNA-seq analysis as previously described (Xing et al., 2016). The sequencing quality of RNA-seq libraries was assessed by FastQC v0.11.4 (http://www.bioinformatics.babraham.ac.uk/projects/fastqc/). RNA-seq libraries were mapped to mouse genome using Tophat (v2.1.0; Trapnell et al., 2009), and the mapped reads were then processed by Cuffdiff (v2.2.1; Trapnell et al., 2010) to estimate expression levels of all genes and identify differentially expressed genes. The expression level of a gene is expressed as a gene-level fragments per kilobase of transcripts per million mapped reads value. The reproducibility of RNA-seq data was evaluated by applying principal component analysis for differential expression genes between biological replicates. UCSC genes from the iGenome mouse mm10 assembly (https://support.illumina.com/sequencing/sequencing_software/igenome.html) were used for gene annotation. The RNA-seq data are deposited at the Gene Expression Omnibus database (accession no. GSE119769).

GSEA

GSEA was performed with GSEA software from the Broad Institute (Subramanian et al., 2005) and used to determine the enrichment of gene sets of interest in *Foxp3*^{Cre}*Tcf7*$^{fl/fl}$*Lef1*$^{fl/fl}$ or *Foxp3*^{Cre} control T reg cells. Either C2 curated gene sets from online resources or custom gene sets were used to analyze the RNA-seq data described above. The custom gene sets including T reg–up and T reg–down signature gene sets which were based on T reg over- and underexpressed genes defined by the Benoist and Mathis groups using over 100 sets of microarray data (Fu et al., 2012). A total of 407 T reg overexpressed and 196 T reg underexpressed microarray IDs were obtained and converted to 295 and 137 unique official gene symbols, respectively, and then used to construct T reg–up and T reg–down signature gene sets.

Gene expression analysis

Splenic CD4$^+$CD25$^+$YFP$^+$ T reg cells were sort-purified from *Foxp3*^{Cre} control and *Foxp3*^{Cre}*Tcf7*$^{fl/fl}$*Lef1*$^{fl/fl}$ mice at 6–8 wk of age (as "young" mice) or at ≥24 wk of age (as "old" mice). The total RNA was extracted from the sorted cells and reverse-transcribed, and qPCR was performed as previously described (Xing et al., 2016). The expression of each gene in a given cell type was first normalized to the *Hprt* housekeeping gene in the same cell type. The gene expression in T reg cells from old *Foxp3*^{Cre} control mice was set at 1, and its relative expression in all other cell types was normalized accordingly. The primer sequences are in Table S1.

ChIP, ChIP-seq, and data processing

CD4$^+$CD25$^+$YFP$^+$ T reg cells and CD4$^+$CD25$^-$YFP$^-$ T conv CD4$^+$ T cells were sort-purified from *Foxp3*^{Cre} control mice. Tcf1-deficient TCRβ$^+$CD4$^+$ T cells were purified from CD4-Cre$^+$*Tcf7*$^{fl/fl}$ mice, and Lef1-deficient TCRβ$^+$CD4$^+$ T cells were purified from CD4-Cre$^+$*Lef1*$^{fl/fl}$ mice as negative controls. The cells were cross-linked with 1% formaldehyde in media for 10 min, processed using truChIP Chromatin Shearing Reagent Kit (Covaris), and sonicated for 5 min on a Covaris S2 ultrasonicator. The sheared chromatin was immunoprecipitated with a homemade anti-Tcf1 antiserum as previously described (Xing et al., 2016) or rabbit anti-mouse Lef1 (C18A7; Cell Signaling Technology). DNA segments from ChIP DNA were end-repaired and ligated to indexed Illumina adaptors followed by low-cycle PCR. The resulting libraries were sequenced with the Illumina HiSeq-2000 platform. The ChIP-seq data are under Gene Expression Omnibus accession nos. GSE119768 and GSE124823.

The sequencing quality of ChIP-seq libraries was assessed by FastQC v0.11.4 (http://www.bioinformatics.babraham.ac.uk/projects/fastqc/). Bowtie2 v2.3.4.1 (Langmead and Salzberg, 2012) was used to align the sequencing reads to the mm10 mouse genome. UCSC genes from the iGenome mouse mm10 assembly were used for gene annotation. Mapped reads were processed with MACS v2.1.1 (Zhang et al., 2008), and Tcf1 peaks in T reg and T conv CD4$^+$ T cells were called by MACS2 (v2.1.1) using Tcf1-deficient CD4$^+$ T cells as a negative control with the stringent setting requiring ≥4-fold enrichment, $P < 10^{-5}$, and FDR < 0.05. Because the Lef1 antibody performs less robustly in ChIP and ChIP-seq analyses, Lef1 peaks in T conv CD4$^+$ T cells were called by MACS2 (v2.1.1) using Lef1-deficient CD4$^+$ T cells as a negative control with $P < 10^{-4}$. Bedtools (v.2.26.0; Quinlan and Hall, 2010) was used to identify peaks that were Tcf1-specific, shared by Tcf1 and Lef1 (requiring at least one base pair overlap), or Lef1-specific. Peaks overlapping with Simple or Satellite Repeats (UCSC RepeatMasker Dec.2011 GRCm38/mm10) for >50% of the peak widths were excluded for analyses in Fig. 8 (A and B).

For Foxp3 binding sites in T reg cells, we used the top 5,039 Foxp3 sites as defined by the Benoist and Mathis groups (Kwon et al., 2017) based on published Foxp3 ChIP-seq data (Samstein et al., 2012; Kitagawa et al., 2017). Bedtools (v.2.26.0; Quinlan and Hall, 2010) was used to identify Tcf1-Foxp3 common peaks, where a Tcf1 binding peak had at least one base pair overlapping with a Foxp3 binding peak.

For motif analysis of the Tcf1 and Foxp3 cooccupied sites in T reg cells, the sequences of peak regions identified by MACS2 were used in MEME-ChIP of the MEME suite for de novo motif discovery using default parameters (Machanick and Bailey, 2011). FIMO (v5.0.1) was used to identify motif occurrences, using P values <0.0001 (Grant et al., 2011). The known motifs of Tcf/Lef and Foxp3 were obtained from the Jaspar 2018 database (http://jaspar.genereg.net/). The matrix ID for Tcf/Lef motif is PB0083.1, and that for Foxp3 motif is MA0850.1.

To differentiate direct versus indirect regulatory effects on T reg cell genes by Tcf1 and/or Foxp3, the differentially expressed genes between *Foxp3*^{Cre} control and *Foxp3*^{Cre} *Tcf7*$^{fl/fl}$*Lef1*$^{fl/fl}$ T reg cells were identified using GSEA. Genes of interest were manually examined for Tcf1 and/or Foxp3 binding peaks within a range of 50 kb upstream of their TSSs to 50 kb downstream of their transcription end sites (i.e., ±50 kb flanking the gene bodies). The genes in each functional category can thus be divided into five subgroups: (1) gene loci harboring overlapping Tcf1 and Foxp3 peaks (called Tcf1-Foxp3 cooccupied genes); (2) gene loci harboring nonoverlapping Tcf1 and Foxp3 peaks (called Tcf1 and Foxp3-associated genes); (3) gene loci harboring Tcf1 peaks only (called Tcf1-only genes); (4) gene loci harboring Foxp3 peaks only (called Foxp3-only genes); and (5) genes containing neither Tcf1 or Foxp3 peaks within the indicated range. The same strategy was applied to Lef1 peaks in T conv cells to infer its shared targets with Tcf1 and cooccupancy with Foxp3.

For validation of Tcf1 binding events, CD4$^+$CD25$^+$YFP$^+$ T reg cells and CD4$^+$CD25$^-$YFP$^-$ T conv CD4$^+$ T cells were sort-purified from *Foxp3*^{Cre} control mice. The cells were processed as above and immunoprecipitated with anti-Tcf1 (C63D9; Cell Signaling Technologies) or normal rabbit IgG, and the immunoprecipitated DNA segments were used for quantification by PCR. To calculate enriched Tcf1 binding, the signal at the genomic region of interest in each Tcf1 ChIP sample was first normalized to that in IgG ChIP, and the relative enrichment by anti-Tcf1 was then normalized to that at the *Hprt* promoter. The primers used are listed in Table S1.

To determine enriched Foxp3 binding, rabbit anti-mouse Foxp3 polyclonal antibody (ab150743; Abcam) was used in ChIP experiments on sorted T reg cells following a published protocol, with *Gmpr* and *Ctla4* as negative and positive controls, respectively (Zheng, 2011).

Statistical analysis

For comparison between two experimental groups, Student's *t* test with two-tailed distribution was used. For multiple group comparisons, one-way ANOVA was used to first determine whether any of the differences among the means are statistically significant, followed by unpaired Student's *t* test to determine the statistical significance between two specific groups. P values of ≤0.05 are considered statistically significant; the following asterisks are used to indicate the level of significance: *, P < 0.05; **, P < 0.01; ***, P < 0.001. P values >0.05 are considered not statistically significant (unmarked or specified as ns).

Online supplementary material

Fig. S1 shows that loss of Tcf1 and/or Lef1 does not perturb thymic T reg cell output. Fig. S2 assesses the suppressive function of Tcf1/Lef1-defiecient T reg cells under various experimental conditions. Fig. S3 shows the impact of Tcf1/Lef1 deficiency on T reg cell transcriptome. Fig. S4 characterizes genome-wide Tcf1 occupancy in T reg cells. Fig. S5 demonstrates functional interplay between Tcf1/Lef1 and Foxp3. Table S1 includes primers for quantitative PCR.

Acknowledgments

We thank Drs. Christophe Benoist and Ricardo Ramirez (Harvard) for sharing the list of top 5,000 Foxp3 binding locations, and Dr. Wenxian Fu (University of California, San Diego, San Diego, CA) for sharing the T reg signature genes. We thank the University of Iowa Flow Cytometry Core facility (J. Fishbaugh, H. Vignes, and G. Rasmussen) for cell sorting.

The Flow Cytometry Core Facility is supported by the Carver College of Medicine/Holden Comprehensive Cancer Center, University of Iowa, the Iowa City Veteran's Administration Medical Center, and the National Center for Research Resources of the National Institutes of Health (1S10 OD016199). This study is supported in part by grants from the National Institutes of Health (AI112579 to H.-H. Xue and AI121080 and AI139874 to H.-H. Xue and W. Peng) and the Veterans Affairs Office of Research and Development Merit Review Program (BX002903A to H.-H. Xue).

The authors declare no competing financial interests.

Author contributions: S. Xing and K. Gai performed all the experiments with help from P. Shao, Xudong Zhao, Xin Zhao, and X. Chen; X. Li and Z. Zeng analyzed RNA-seq and ChIP-seq data under supervision of W. Peng; W.J. Paradee designed and supervised generation of *Prdm1* mutant mice using CRISPR/Cas9; D.K. Meyerholz provided expertise in histology studies; and H.-H. Xue conceived the project, supervised the overall study, and wrote the paper with W. Peng. All authors edited the paper.

Submitted: 24 October 2018
Revised: 14 January 2019
Accepted: 14 February 2019

References

Arce, L., N.N. Yokoyama, and M.L. Waterman. 2006. Diversity of LEF/TCF action in development and disease. *Oncogene.* 25:7492–7504. https://doi.org/10.1038/sj.onc.1210056

Baron, U., S. Floess, G. Wieczorek, K. Baumann, A. Grützkau, J. Dong, A. Thiel, T.J. Boeld, P. Hoffmann, M. Edinger, et al. 2007. DNA demethylation in the human FOXP3 locus discriminates regulatory T cells from activated FOXP3(+) conventional T cells. *Eur. J. Immunol.* 37:2378–2389. https://doi.org/10.1002/eji.200737594

Barra, M.M., D.M. Richards, J. Hansson, A.C. Hofer, M. Delacher, J. Hettinger, J. Krijgsveld, and M. Feuerer. 2015. Transcription Factor 7 Limits Regulatory T Cell Generation in the Thymus. *J. Immunol.* 195:3058–3070. https://doi.org/10.4049/jimmunol.1500821

Choi, Y.S., J.A. Gullicksrud, S. Xing, Z. Zeng, Q. Shan, F. Li, P.E. Love, W. Peng, H.H. Xue, and S. Crotty. 2015. LEF-1 and TCF-1 orchestrate T(FH) differentiation by regulating differentiation circuits upstream of the transcriptional repressor Bcl6. *Nat. Immunol.* 16:980–990. https://doi.org/10.1038/ni.3226

Delacher, M., L. Schreiber, D.M. Richards, C. Farah, M. Feuerer, and J. Huehn. 2014. Transcriptional control of regulatory T cells. *Curr. Top. Microbiol. Immunol.* 381:83–124.

De Obaldia, M.E., and A. Bhandoola. 2015. Transcriptional regulation of innate and adaptive lymphocyte lineages. *Annu. Rev. Immunol.* 33: 607–642. https://doi.org/10.1146/annurev-immunol-032414-112032

Ding, Y., S. Shen, A.C. Lino, M.A. Curotto de Lafaille, and J.J. Lafaille. 2008. Beta-catenin stabilization extends regulatory T cell survival and induces anergy in nonregulatory T cells. *Nat. Med.* 14:162–169. https://doi.org/10.1038/nm1707

Emmanuel, A.O., S. Arnovitz, L. Haghi, P.S. Mathur, S. Mondal, J. Quandt, M. K. Okoreeh, M. Maienschein-Cline, K. Khazaie, M. Dose, and F. Gounari. 2018. TCF-1 and HEB cooperate to establish the epigenetic and transcription profiles of $CD4^+CD8^+$ thymocytes. *Nat. Immunol.* 19:1366–1378. https://doi.org/10.1038/s41590-018-0254-4

Fu, W., A. Ergun, T. Lu, J.A. Hill, S. Haxhinasto, M.S. Fassett, R. Gazit, S. Adoro, L. Glimcher, S. Chan, et al. 2012. A multiply redundant genetic switch 'locks in' the transcriptional signature of regulatory T cells. *Nat. Immunol.* 13:972–980. https://doi.org/10.1038/ni.2420

Germar, K., M. Dose, T. Konstantinou, J. Zhang, H. Wang, C. Lobry, K.L. Arnett, S.C. Blacklow, I. Aifantis, J.C. Aster, and F. Gounari. 2011. T-cell factor 1 is a gatekeeper for T-cell specification in response to Notch signaling. *Proc. Natl. Acad. Sci. USA.* 108:20060–20065. https://doi.org/10.1073/pnas.1110230108

Goldrath, A.W., C.J. Luckey, R. Park, C. Benoist, and D. Mathis. 2004. The molecular program induced in T cells undergoing homeostatic proliferation. *Proc. Natl. Acad. Sci. USA.* 101:16885–16890. https://doi.org/10.1073/pnas.0407417101

Grant, C.E., T.L. Bailey, and W.S. Noble. 2011. FIMO: scanning for occurrences of a given motif. *Bioinformatics.* 27:1017–1018. https://doi.org/10.1093/bioinformatics/btr064

Guo, Z., M. Dose, D. Kovalovsky, R. Chang, J. O'Neil, A.T. Look, H. von Boehmer, K. Khazaie, and F. Gounari. 2007. Beta-catenin stabilization stalls the transition from double-positive to single-positive stage and predisposes thymocytes to malignant transformation. *Blood.* 109: 5463–5472. https://doi.org/10.1182/blood-2006-11-059071

Hansen, W., K. Loser, A.M. Westendorf, D. Bruder, S. Pfoertner, C. Siewert, J. Huehn, S. Beissert, and J. Buer. 2006. G protein-coupled receptor 83 overexpression in naive CD4+CD25- T cells leads to the induction of Foxp3+ regulatory T cells in vivo. *J. Immunol.* 177:209–215. https://doi.org/10.4049/jimmunol.177.1.209

He, B., S. Xing, C. Chen, P. Gao, L. Teng, Q. Shan, J.A. Gullicksrud, M.D. Martin, S. Yu, J.T. Harty, et al. 2016. $CD8^+$ T Cells Utilize Highly Dynamic Enhancer Repertoires and Regulatory Circuitry in Response to Infections. *Immunity.* 45:1341–1354. https://doi.org/10.1016/j.immuni.2016.11.009

Hill, J.A., M. Feuerer, K. Tash, S. Haxhinasto, J. Perez, R. Melamed, D. Mathis, and C. Benoist. 2007. Foxp3 transcription-factor-dependent and -independent regulation of the regulatory T cell transcriptional signature. *Immunity.* 27:786–800. https://doi.org/10.1016/j.immuni.2007.09.010

Hori, S. 2012. The Foxp3 interactome: a network perspective of T(reg) cells. *Nat. Immunol.* 13:943–945. https://doi.org/10.1038/ni.2424

Hossain, M.B., H. Hosokawa, A. Hasegawa, H. Watarai, M. Taniguchi, M. Yamashita, and T. Nakayama. 2008. Lymphoid enhancer factor interacts with GATA-3 and controls its function in T helper type 2 cells. *Immunology.* 125:377–386. https://doi.org/10.1111/j.1365-2567.2008.02854.x

Intlekofer, A.M., N. Takemoto, E.J. Wherry, S.A. Longworth, J.T. Northrup, V. R. Palanivel, A.C. Mullen, C.R. Gasink, S.M. Kaech, J.D. Miller, et al. 2005. Effector and memory CD8+ T cell fate coupled by T-bet and eomesodermin. *Nat. Immunol.* 6:1236–1244. https://doi.org/10.1038/ni1268

Kalekar, L.A., S.E. Schmiel, S.L. Nandiwada, W.Y. Lam, L.O. Barsness, N. Zhang, G.L. Stritesky, D. Malhotra, K.E. Pauken, J.L. Linehan, et al. 2016. CD4(+) T cell anergy prevents autoimmunity and generates regulatory T cell precursors. *Nat. Immunol.* 17:304–314. https://doi.org/10.1038/ni.3331

Kitagawa, Y., N. Ohkura, Y. Kidani, A. Vandenbon, K. Hirota, R. Kawakami, K. Yasuda, D. Motooka, S. Nakamura, M. Kondo, et al. 2017. Guidance of regulatory T cell development by Satb1-dependent super-enhancer establishment. *Nat. Immunol.* 18:173–183. https://doi.org/10.1038/ni.3646

Koch, M.A., G. Tucker-Heard, N.R. Perdue, J.R. Killebrew, K.B. Urdahl, and D. J. Campbell. 2009. The transcription factor T-bet controls regulatory T cell homeostasis and function during type 1 inflammation. *Nat. Immunol.* 10:595–602. https://doi.org/10.1038/ni.1731

Koch, M.A., K.R. Thomas, N.R. Perdue, K.S. Smigiel, S. Srivastava, and D.J. Campbell. 2012. T-bet(+) Treg cells undergo abortive Th1 cell differentiation due to impaired expression of IL-12 receptor β2. *Immunity.* 37: 501–510. https://doi.org/10.1016/j.immuni.2012.05.031

Kwon, H.K., H.M. Chen, D. Mathis, and C. Benoist. 2017. Different molecular complexes that mediate transcriptional induction and repression by FoxP3. *Nat. Immunol.* 18:1238–1248. https://doi.org/10.1038/ni.3835

Langmead, B., and S.L. Salzberg. 2012. Fast gapped-read alignment with Bowtie 2. *Nat. Methods.* 9:357–359. https://doi.org/10.1038/nmeth.1923

Levine, A.G., A. Mendoza, S. Hemmers, B. Moltedo, R.E. Niec, M. Schizas, B.E. Hoyos, E.V. Putintseva, A. Chaudhry, S. Dikiy, et al. 2017. Stability and function of regulatory T cells expressing the transcription factor T-bet. *Nature.* 546:421–425. https://doi.org/10.1038/nature22360

Li, F., Z. Zeng, S. Xing, J.A. Gullicksrud, Q. Shan, J. Choi, V.P. Badovinac, S. Crotty, W. Peng, and H.H. Xue. 2018. Ezh2 programs T_{FH} differentiation by integrating phosphorylation-dependent activation of Bcl6 and polycomb-dependent repression of p19Arf. *Nat. Commun.* 9:5452. https://doi.org/10.1038/s41467-018-07853-z

Lu, L., J. Barbi, and F. Pan. 2017. The regulation of immune tolerance by FOXP3. *Nat. Rev. Immunol.* 17:703–717. https://doi.org/10.1038/nri.2017.75

Luis, T.C., B.A. Naber, P.P. Roozen, M.H. Brugman, E.F. de Haas, M. Ghazvini, W.E. Fibbe, J.J. van Dongen, R. Fodde, and F.J. Staal. 2011. Canonical wnt signaling regulates hematopoiesis in a dosage-dependent fashion. *Cell Stem Cell.* 9:345–356. https://doi.org/10.1016/j.stem.2011.07.017

Machanick, P., and T.L. Bailey. 2011. MEME-ChIP: motif analysis of large DNA datasets. *Bioinformatics.* 27:1696–1697. https://doi.org/10.1093/bioinformatics/btr189

Meyerholz, D.K., and A.P. Beck. 2018. Principles and approaches for reproducible scoring of tissue stains in research. *Lab. Invest.* 98:844–855. https://doi.org/10.1038/s41374-018-0057-0

Meyerholz, D.K., J.C. Sieren, A.P. Beck, and H.A. Flaherty. 2018. Approaches to Evaluate Lung Inflammation in Translational Research. *Vet. Pathol.* 55:42–52. https://doi.org/10.1177/0300985817726117

Morgan, M.E., B. Zheng, P.J. Koelink, H.J. van de Kant, L.C. Haazen, M. van Roest, J. Garssen, G. Folkerts, and A.D. Kraneveld. 2013. New perspective on dextran sodium sulfate colitis: antigen-specific T cell development during intestinal inflammation. *PLoS One.* 8:e69936. https://doi.org/10.1371/journal.pone.0069936

Okamura, R.M., M. Sigvardsson, J. Galceran, S. Verbeek, H. Clevers, and R. Grosschedl. 1998. Redundant regulation of T cell differentiation and TCRalpha gene expression by the transcription factors LEF-1 and TCF-1. *Immunity.* 8:11–20. https://doi.org/10.1016/S1074-7613(00)80454-9

Pan, F., H. Yu, E.V. Dang, J. Barbi, X. Pan, J.F. Grosso, D. Jinasena, S.M. Sharma, E.M. McCadden, D. Getnet, et al. 2009. Eos mediates Foxp3-dependent gene silencing in CD4+ regulatory T cells. *Science.* 325: 1142–1146. https://doi.org/10.1126/science.1176077

Quinlan, A.R., and I.M. Hall. 2010. BEDTools: a flexible suite of utilities for comparing genomic features. *Bioinformatics.* 26:841–842. https://doi.org/10.1093/bioinformatics/btq033

Ramsdell, F., and S.F. Ziegler. 2014. FOXP3 and scurfy: how it all began. *Nat. Rev. Immunol.* 14:343–349. https://doi.org/10.1038/nri3650

Rubtsov, Y.P., J.P. Rasmussen, E.Y. Chi, J. Fontenot, L. Castelli, X. Ye, P. Treuting, L. Siewe, A. Roers, W.R. Henderson Jr., et al. 2008. Regulatory T cell-derived interleukin-10 limits inflammation at environmental interfaces. *Immunity.* 28:546–558. https://doi.org/10.1016/j.immuni.2008.02.017

Rudra, D., P. deRoos, A. Chaudhry, R.E. Niec, A. Arvey, R.M. Samstein, C. Leslie, S.A. Shaffer, D.R. Goodlett, and A.Y. Rudensky. 2012. Transcription factor Foxp3 and its protein partners form a complex regulatory network. *Nat. Immunol.* 13:1010–1019. https://doi.org/10.1038/ni.2402

Sakaguchi, S., D.A. Vignali, A.Y. Rudensky, R.E. Niec, and H. Waldmann. 2013. The plasticity and stability of regulatory T cells. *Nat. Rev. Immunol.* 13:461–467. https://doi.org/10.1038/nri3464

Samstein, R.M., A. Arvey, S.Z. Josefowicz, X. Peng, A. Reynolds, R. Sandstrom, S. Neph, P. Sabo, J.M. Kim, W. Liao, et al. 2012. Foxp3 exploits a pre-existent enhancer landscape for regulatory T cell lineage specification. *Cell.* 151:153–166. https://doi.org/10.1016/j.cell.2012.06.053

Shan, Q., Z. Zeng, S. Xing, F. Li, S.M. Hartwig, J.A. Gullicksrud, S.P. Kurup, N. Van Braeckel-Budimir, Y. Su, M.D. Martin, et al. 2017. The transcription factor Runx3 guards cytotoxic $CD8^+$ effector T cells against deviation towards follicular helper T cell lineage. *Nat. Immunol.* 18:931–939. https://doi.org/10.1038/ni.3773

Staal, F.J., and J.M. Sen. 2008. The canonical Wnt signaling pathway plays an important role in lymphopoiesis and hematopoiesis. *Eur. J. Immunol.* 38: 1788–1794. https://doi.org/10.1002/eji.200738118

Steinke, F.C., and H.H. Xue. 2014. From inception to output, Tcf1 and Lef1 safeguard development of T cells and innate immune cells. *Immunol. Res.* 59:45–55. https://doi.org/10.1007/s12026-014-8545-9

Steinke, F.C., S. Yu, X. Zhou, B. He, W. Yang, B. Zhou, H. Kawamoto, J. Zhu, K. Tan, and H.H. Xue. 2014. TCF-1 and LEF-1 act upstream of Th-POK to promote the CD4(+) T cell fate and interact with Runx3 to silence Cd4 in CD8(+) T cells. *Nat. Immunol.* 15:646–656. https://doi.org/10.1038/ni.2897

Subramanian, A., P. Tamayo, V.K. Mootha, S. Mukherjee, B.L. Ebert, M.A. Gillette, A. Paulovich, S.L. Pomeroy, T.R. Golub, E.S. Lander, and J.P. Mesirov. 2005. Gene set enrichment analysis: a knowledge-based approach for interpreting genome-wide expression profiles. *Proc. Natl. Acad. Sci. USA.* 102: 15545–15550. https://doi.org/10.1073/pnas.0506580102

Sumida, T., M.R. Lincoln, C.M. Ukeje, D.M. Rodriguez, H. Akazawa, T. Noda, A.T. Naito, I. Komuro, M. Dominguez-Villar, and D.A. Hafler. 2018. Activated β-catenin in Foxp3$^+$ regulatory T cells links inflammatory environments to autoimmunity. *Nat. Immunol.* 19:1391–1402. https://doi.org/10.1038/s41590-018-0236-6

Trapnell, C., L. Pachter, and S.L. Salzberg. 2009. TopHat: discovering splice junctions with RNA-Seq. *Bioinformatics.* 25:1105–1111. https://doi.org/10.1093/bioinformatics/btp120

Trapnell, C., B.A. Williams, G. Pertea, A. Mortazavi, G. Kwan, M.J. van Baren, S.L. Salzberg, B.J. Wold, and L. Pachter. 2010. Transcript assembly and quantification by RNA-Seq reveals unannotated transcripts and isoform switching during cell differentiation. *Nat. Biotechnol.* 28:511–515. https://doi.org/10.1038/nbt.1621

van Loosdregt, J., V. Fleskens, M.M. Tiemessen, M. Mokry, R. van Boxtel, J. Meerding, C.E. Pals, D. Kurek, M.R. Baert, E.M. Delemarre, et al. 2013. Canonical Wnt signaling negatively modulates regulatory T cell function. *Immunity.* 39:298–310. https://doi.org/10.1016/j.immuni.2013.07.019

Weber, B.N., A.W. Chi, A. Chavez, Y. Yashiro-Ohtani, Q. Yang, O. Shestova, and A. Bhandoola. 2011. A critical role for TCF-1 in T-lineage specification and differentiation. *Nature.* 476:63–68. https://doi.org/10.1038/nature10279

Wu, T., H.M. Shin, E.A. Moseman, Y. Ji, B. Huang, C. Harly, J.M. Sen, L.J. Berg, L. Gattinoni, D.B. McGavern, and P.L. Schwartzberg. 2015. TCF1 Is Required for the T Follicular Helper Cell Response to Viral Infection. *Cell Reports.* 12:2099–2110. https://doi.org/10.1016/j.celrep.2015.08.049

Xie, H., Z. Huang, M.S. Sadim, and Z. Sun. 2005. Stabilized beta-catenin extends thymocyte survival by up-regulating Bcl-xL. *J. Immunol.* 175: 7981–7988. https://doi.org/10.4049/jimmunol.175.12.7981

Xing, S., F. Li, Z. Zeng, Y. Zhao, S. Yu, Q. Shan, Y. Li, F.C. Phillips, P.K. Maina, H.H. Qi, et al. 2016. Tcf1 and Lef1 transcription factors establish CD8(+) T cell identity through intrinsic HDAC activity. *Nat. Immunol.* 17: 695–703. https://doi.org/10.1038/ni.3456

Xing, S., P. Shao, F. Li, X. Zhao, W. Seo, J.C. Wheat, S. Ramasamy, J. Wang, X. Li, W. Peng, et al. 2018. Tle corepressors are differentially partitioned to instruct CD8$^+$ T cell lineage choice and identity. *J. Exp. Med.* 215: 2211–2226. https://doi.org/10.1084/jem.20171514

Xu, L., Y. Cao, Z. Xie, Q. Huang, Q. Bai, X. Yang, R. He, Y. Hao, H. Wang, T. Zhao, et al. 2015. The transcription factor TCF-1 initiates the differentiation of T(FH) cells during acute viral infection. *Nat. Immunol.* 16: 991–999. https://doi.org/10.1038/ni.3229

Xue, H.H., and D.M. Zhao. 2012. Regulation of mature T cell responses by the Wnt signaling pathway. *Ann. N. Y. Acad. Sci.* 1247:16–33. https://doi.org/10.1111/j.1749-6632.2011.06302.x

Yu, F., S. Sharma, J. Edwards, L. Feigenbaum, and J. Zhu. 2015. Dynamic expression of transcription factors T-bet and GATA-3 by regulatory T cells maintains immunotolerance. *Nat. Immunol.* 16:197–206. https://doi.org/10.1038/ni.3053

Yu, Q., A. Sharma, S.Y. Oh, H.G. Moon, M.Z. Hossain, T.M. Salay, K.E. Leeds, H. Du, B. Wu, M.L. Waterman, et al. 2009. T cell factor 1 initiates the T helper type 2 fate by inducing the transcription factor GATA-3 and repressing interferon-gamma. *Nat. Immunol.* 10:992–999. https://doi.org/10.1038/ni.1762

Yu, S., X. Zhou, F.C. Steinke, C. Liu, S.C. Chen, O. Zagorodna, X. Jing, Y. Yokota, D.K. Meyerholz, C.G. Mullighan, et al. 2012. The TCF-1 and LEF-1 transcription factors have cooperative and opposing roles in T cell development and malignancy. *Immunity.* 37:813–826. https://doi.org/10.1016/j.immuni.2012.08.009

Zhang, J., Z. He, S. Sen, F. Wang, Q. Zhang, and Z. Sun. 2018. TCF-1 Inhibits IL-17 Gene Expression To Restrain Th17 Immunity in a Stage-Specific Manner. *J. Immunol.* 200:3397–3406. https://doi.org/10.4049/jimmunol.1800193

Zhang, Y., T. Liu, C.A. Meyer, J. Eeckhoute, D.S. Johnson, B.E. Bernstein, C. Nusbaum, R.M. Myers, M. Brown, W. Li, and X.S. Liu. 2008. Model-based analysis of ChIP-Seq (MACS). *Genome Biol.* 9:R137. https://doi.org/10.1186/gb-2008-9-9-r137

Zhao, D.M., and H.H. Xue. 2017. MLL4 keeps Foxp3 in the loop. *Nat. Immunol.* 18:957–958. https://doi.org/10.1038/ni.3811

Zhao, D.M., A.M. Thornton, R.J. DiPaolo, and E.M. Shevach. 2006. Activated CD4+CD25+ T cells selectively kill B lymphocytes. *Blood.* 107:3925–3932. https://doi.org/10.1182/blood-2005-11-4502

Zheng, Y. 2011. ChIP-on-chip for FoxP3. *Methods Mol. Biol.* 707:71–82. https://doi.org/10.1007/978-1-61737-979-6_6

Zheng, Y., S. Josefowicz, A. Chaudhry, X.P. Peng, K. Forbush, and A.Y. Rudensky. 2010. Role of conserved non-coding DNA elements in the Foxp3 gene in regulatory T-cell fate. *Nature.* 463:808–812. https://doi.org/10.1038/nature08750

Zhou, X., and H.H. Xue. 2012. Cutting edge: generation of memory precursors and functional memory CD8+ T cells depends on T cell factor-1 and lymphoid enhancer-binding factor-1. *J. Immunol.* 189:2722–2726. https://doi.org/10.4049/jimmunol.1201150

Zhou, X., S. Yu, D.M. Zhao, J.T. Harty, V.P. Badovinac, and H.H. Xue. 2010. Differentiation and persistence of memory CD8(+) T cells depend on T cell factor 1. *Immunity.* 33:229–240. https://doi.org/10.1016/j.immuni.2010.08.002